

---

# MITIGATING OBJECT HALLUCINATION IN LARGE VISION-LANGUAGE MODELS VIA IMAGE-GROUNDED GUIDANCE

Linxi Zhao<sup>\*1</sup>, Yihe Deng<sup>\*2</sup>, Weitong Zhang<sup>2</sup>, Quanquan Gu<sup>2</sup>

<sup>1</sup>Cornell University

<sup>2</sup>University of California, Los Angeles

## ABSTRACT

The advancement of Large Vision-Language Models (LVLMs) has increasingly highlighted the critical issue of their tendency to hallucinate non-existing objects in the images. To address this issue, previous works focused on using specially curated datasets or powerful LLMs (e.g., GPT-3.5) to rectify the outputs of LVLMs. However, these approaches require either expensive training/fine-tuning or API access to advanced LLMs for post-generation correction. In response to these limitations, we propose **Mitigating hallucinAtion via image-gRounded guIdaNcE** (MARINE), a framework that is both *training-free* and *API-free*. MARINE effectively and efficiently reduces object hallucinations during inference by introducing image-grounded guidance to LVLMs. This is achieved by leveraging open-source vision models to extract object-level information, thereby enhancing the precision of LVLM-generated content. Our framework’s flexibility further allows for the integration of multiple vision models, enabling more reliable and robust object-level guidance. Through comprehensive evaluations across 5 popular LVLMs with diverse evaluation metrics and benchmarks, we demonstrate the effectiveness of MARINE, which even outperforms existing fine-tuning-based methods. Remarkably, it reduces hallucinations consistently in GPT-4V-assisted evaluation while maintaining the detailedness of LVLMs’ generations.

## 1 INTRODUCTION

The advent of Large Language Models (LLMs) has motivated advancements in extending their remarkable capabilities to multimodal data. Grounded in the development of pre-trained vision-language models (Radford et al., 2021; Jia et al., 2021; Alayrac et al., 2022) that align visual and textual embedding spaces, Large Vision Language Models (LVLMs) have gained substantial attention in both architectural development (Liu et al., 2023d; Zhu et al., 2023; Ye et al., 2023; Dai et al., 2023a; Gao et al., 2023), alignment (Yu et al., 2024; Zhou et al., 2024; Deng et al., 2024) and benchmarking datasets (Xu et al., 2023; Lu et al., 2024; Zhang et al., 2024). However, similar to the hallucination issues in textual LLMs (Ji et al., 2023), where irrelevant content is generated with input prompts, LVLMs face a specific challenge known as object hallucination: generating non-existing objects for a given image (Li et al., 2023b; Wang et al., 2023b; Zhou et al., 2023; Fu et al., 2023; Lovenia et al., 2023; Jing et al., 2023). Such a problem is particularly concerning as it compromises the model’s accuracy and reliability, especially considering the growing application of LVLMs to safety-critical downstream tasks such as medical imaging (Chambon et al., 2022; Bazi et al., 2023).

In response to the pressing issue of object hallucinations in LVLMs, early attempts (Liu et al., 2023a;b; Gunjal et al., 2023; Wang et al., 2023a) focused on addressing the bias by curating high-quality datasets for fine-tuning or leveraging advanced GPT queries (Yin et al., 2023), such as GPT-4, to post-process the generated captions. However, these methods can be infeasible to implement. For instance, creating extensive, high-quality datasets for fine-tuning LVLMs is costly and requires significant human annotation. Additionally, relying on advanced GPT models for post-processing is expensive and can raise privacy concerns, especially in sensitive fields like medical imaging. Most importantly, these approaches do not address the *intrinsic* causes of object hallucination in LVLMs. Specifically, fine-tuning simply provides more data for the LVLM to learn, which can lead to overfitting to a

---

<sup>\*</sup>Equal contribution.

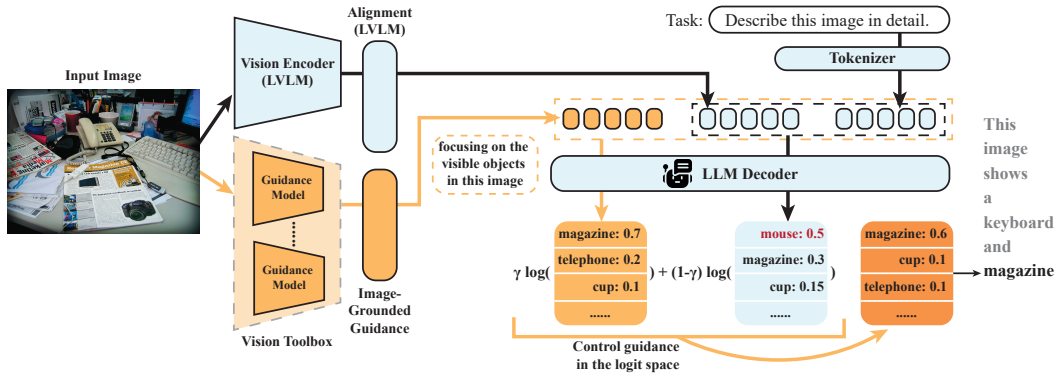


Figure 1: Illustration of MARINE framework, which introduces a vision toolbox with one or multiple guidance models to enrich the visual context of the original LVLM. The output logits are controlled to place more importance on the guided generation with the guidance strength  $\gamma$ .

particular dataset, as seen with methods like LURE (Zhou et al., 2023). Post-processing methods may also introduce new hallucinations, as they do not inherently correct the root cause of hallucinations in LLMs or LVLMs but just overwrite the generated response.

In this paper, we investigate the intrinsic causes of object hallucination in LVLMs. Specifically, these deficiencies may stem from the three main components of the LVLMs: 1) insufficient visual context provided by the visual encoder (Zhang et al., 2023b), 2) misalignment between the vision and text domains, and 3) inherent hallucinations common in general language models. To address the first two LVLM-specific causes, we introduce Mitigating hallucinAtion via image-gRounded guIdaNcE (MARINE). MARINE mitigates hallucination issues arising from the visual encoder and domain misalignment by leveraging external guidance from image-grounded models, such as object detection models. Our approach leverages the inherent advantage of these image-grounded models, which are specifically designed and trained for more detailed visual information extraction. These models provide higher quality, fine-grained visual encoding compared to the standard visual encoders in LVLMs, which are primarily optimized for grasping the overall context of an image. Furthermore, we integrate the guidance from image-grounded models into text descriptions, allowing the LVLM to process the information without requiring additional alignment procedures. As a result, MARINE is a training-free, API-free\* method that addresses object hallucination at inference time by targeting its two root causes.

As shown in Figure 1, MARINE incorporates one or more image-grounding models to enrich the visual context of LVLMs. The guidance are then aggregated as prompt input to the LLM decoder to improve the response quality. Empirical evaluations are conducted on five widely-recognized LVLMs across benchmarks including MSCOCO (Lin et al., 2014), LLaVA-QA90 task (Liu et al., 2023d), A-OKVQA (Schwenk et al., 2022), and GQA (Hudson & Manning, 2019). We present results based on guidance from an aggregated source of DETection TRansformer (DETR) (Carion et al., 2020) and RAM++ (Huang et al., 2023b). We also include ideal results based on ground truth object oracle, denoted as MARINE-Truth. Our experimental results demonstrate that, in comparison with state-of-the-art algorithms, MARINE exhibits further reduced hallucination, as measured by popular hallucination metrics such as CHAIR (Rohrbach et al., 2018) and POPE (Li et al., 2023b), as well as additional metrics considered in this study including the recall and GPT-4V’s evaluation of the responses. These results confirm that MARINE can effectively mitigate object hallucinations without requiring additional training resources or access to advanced LLMs. To summarize, our contribution are listed as follows:

- We introduce MARINE, a universal framework and aggregating a toolbox of image-grounded visual models to guide the generation process of LVLMs. MARINE leverages the intrinsic advantages of these visual models in providing the detailed information of the input image and help mitigate the hallucinations in LVLMs.

\*The term “API-free” in denotes the elimination of any need for API calls to OpenAI. We note that Woodpecker requires 3-5k input tokens for an API call to each short captioning task.

- Through extensive evaluations on various datasets, we demonstrate that MARINE consistently outperform the baselines in hallucination mitigation while maintaining overall performance across multiple tasks (image captioning, VQA).
- MARINE provides a favorable trade-off between latency and accuracy, with the lowest computational overhead compared to existing baselines. The minimal increase in latency comparing to the baselines, combined with the high accuracy of our results, positions MARINE as a practical and scalable solution for real-world applications without significant computational cost.

## 2 RELATED WORK

Since the introduction of recent Large Vision-Language Models (LVLMs) (Liu et al., 2023d; Zhu et al., 2023; Ye et al., 2023; Dai et al., 2023a; Gao et al., 2023), the hallucination phenomenon in these models has gathered significant attention in the research community. This issue was first highlighted by Li et al. (2023b) with subsequent studies (Wang et al., 2023b; Zhou et al., 2023; Fu et al., 2023; Lovenia et al., 2023) that, LVLMs exhibit similar hallucination problems as the textual LLMs. Notably, different from textual LLMs, LVLMs are prone to a unique type of hallucination called ‘object hallucination’ (Rohrbach et al., 2018), where the model falsely perceives the presence of non-existent objects in images. In response to object hallucination problems, efforts have been made to mitigate object hallucination in smaller image captioning models (Biten et al., 2022; Dai et al., 2023b). Regarding the recent development of LVLMs, several works (Liu et al., 2023b; Gunjal et al., 2023) proposed vision-language fine-tuning datasets aimed for improved robustness. Wang et al. (2023a) leveraged the vision-language model to generate more diverse instruction-tuning data and iteratively correct the inaccuracies in data. Zhai et al. (2023) introduced a GPT-4 assisted evaluation method and also a fine-tuning strategy using the MSCOCO dataset. Most related to our setting, Yin et al. (2023) proposed Woodepecker, a five-stage training-free method eventually leveraging GPT-3.5 API for hallucination correction. Concurrently, Leng et al. (2023) introduced Visual Contrastive Decoding (VCD), a technique that applies noise to image inputs and penalizes logit outputs of these corrupted images. Huang et al. (2023a) enhanced beam-search decoding with the Over-trust Penalty and Retrospection-Allocation Strategy (OPERA), which penalizes over-trust and refines token selection based on previous outputs. HALC (Chen et al., 2024) employs adaptive focal-contrast decoding to encourage LVLMs to focus on fine-grained visual information, while using a computationally intensive beam search algorithm. In contrast to these approaches, MARINE incorporates additional visual guidance in the generation process, offering an efficient and effective approach for hallucination mitigation in LVLMs.

## 3 PRELIMINARIES

**Notation.** We use lower case letters, lower case bold face letters, and upper case bold face letters to denote scalars, vectors, and matrices respectively. We use the symbol  $p$  to represent the conditional probability of LLM’s response. And we denote the sequence of tokens generated before the  $t$ -th token as  $\mathbf{y}_{<t} = [y_1, \dots, y_{t-1}]$  for  $t > 1$ .  $\mathbf{y}_{<t}$  is an empty sequence when  $t = 1$ .

**Generative language models.** Let  $p_\theta$  denotes an LLM parameterized by  $\theta$ . Consider a sequence  $\mathbf{x} = [x_1, \dots, x_n]$  as the input prompt, where each  $x_i$  is a token from a predefined vocabulary. The LLM then generates the response sequence  $\mathbf{y} = [y_1, \dots, y_m]$  by sampling from the conditional probability distribution  $p_\theta(\cdot|\mathbf{x})$ , where  $y_t$  denotes individual token for  $1 \leq t \leq m$ . The conditional distribution  $p_\theta(\mathbf{y}|\mathbf{x})$  can therefore be expressed as  $p_\theta(\mathbf{y}|\mathbf{x}) = \prod_{t=1}^m p_\theta(y_t|\mathbf{x}, \mathbf{y}_{<t})$ , where  $\mathbf{y}_{<t} = [y_1, \dots, y_{t-1}]$  for  $t > 1$  and is empty for  $t = 1$ . In the case of LVLMs, visual tokens  $\mathbf{v} = [v_1, \dots, v_k]$  are additionally included. These tokens are generated from a pre-trained visual encoder and mapped into the token space through a linear projection. The conditional distribution of output  $\mathbf{y}$  given the visual tokens  $\mathbf{v}$  and textual prompt  $\mathbf{x}$  is expressed as  $p_\theta(\mathbf{y}|\mathbf{v}, \mathbf{x}) = \prod_{t=1}^m p_\theta(y_t|\mathbf{v}, \mathbf{x}, \mathbf{y}_{<t})$ , where  $p_\theta$  is approximated by LVLMs.

## 4 METHOD

The existing architecture of LVLMs is usually composed of a visual encoder, a visual and textual domain alignment layer, and the LLM itself. Therefore, besides the inherent language priors of LLMs (Biten et al., 2022), object hallucination may arise from (1) deficiencies in the visual encoder providing insufficient visual information (Zhang et al., 2023b) and (2) misalignment between the visual and textual domains. To mitigate object hallucinations, we introduce MARINE, a framework containing two major components to address the aforementioned challenges: (1) introducing additional visual information from a set of vision models and (2) using the additional aggregated visual features to guide the LVLM’s generation. In Figure 1, we present the framework overview.

---

#### 4.1 VISUAL GUIDANCE FROM IMAGE-GROUNDED FEATURES

To introduce image-grounded guidance to mitigate hallucinations, our approach integrates additional object detection models, which differ from the visual encoders used in LVLm that are usually pre-trained from CLIP (Radford et al., 2021). This integration leverages the object detection models to extract detailed visual information from images. Upon acquiring these extra visual information from different image-grounded models, we aggregate and translate the collected information into textual information. This aggregation can be done by the language model (Lin et al., 2023a) or rule based algorithm (Bird et al., 2009). Such an information aggregation is effective and efficient, as it eliminates the necessity of fine-tuning the alignment layer while retaining the rich information encoded by various of image grounding models. We subsequently employ a simple prompt “focusing on the visible objects in this image:” and concatenate it with the aggregated object information, denoted as the guidance prompt  $\mathbf{c}$ .

#### 4.2 GUIDED TEXT GENERATION WITH VISUAL INFORMATION

We tackle the object hallucination problem of LVLms by specifically placing importance on the additional image-grounded information we introduced. In addition to the visual tokens  $\mathbf{v}$  extracted from the original LVLm and textual prompt  $\mathbf{x}$ , we extract the auxiliary visual tokens  $\mathbf{c}$  from the additional guidance models. The generation of the  $t$ -th token in the output  $\mathbf{y}$  of our classifier-free guided LVLm  $p_\theta$  is expressed as

$$\hat{p}_\theta(y_t|\mathbf{v}, \mathbf{c}, \mathbf{x}, \mathbf{y}_{<t}) \propto p_\theta(y_t|\mathbf{v}, \mathbf{c}, \mathbf{x}, \mathbf{y}_{<t})^\gamma / p_\theta(y_t|\mathbf{v}, \mathbf{x}, \mathbf{y}_{<t})^{\gamma-1},$$

where  $\mathbf{c}$  denotes our control guidance and  $\gamma$  is the control strength. The sampling of output is:

$$\hat{p}_\theta(\mathbf{y}|\mathbf{v}, \mathbf{c}, \mathbf{x}) = \prod_{t=1}^m \hat{p}_\theta(y_t|\mathbf{v}, \mathbf{c}, \mathbf{x}, \mathbf{y}_{<t}) \propto \prod_{t=1}^m \frac{p_\theta(y_t|\mathbf{v}, \mathbf{c}, \mathbf{x}, \mathbf{y}_{<t})^\gamma}{p_\theta(y_t|\mathbf{v}, \mathbf{x}, \mathbf{y}_{<t})^{\gamma-1}} = \frac{p_\theta(\mathbf{y}|\mathbf{v}, \mathbf{c}, \mathbf{x})^\gamma}{p_\theta(\mathbf{y}|\mathbf{v}, \mathbf{x})^{\gamma-1}}.$$

We can further view MARINE in the logit space, where the  $t$ -th token is therefore sampled by

$$\log \hat{p}_\theta(y_t|\mathbf{v}, \mathbf{c}, \mathbf{x}, \mathbf{y}_{<t}) = \gamma \log p_\theta(y_t|\mathbf{v}, \mathbf{c}, \mathbf{x}, \mathbf{y}_{<t}) + (1 - \gamma) \log p_\theta(y_t|\mathbf{v}, \mathbf{x}, \mathbf{y}_{<t}).$$

This linear combination of logits implies that the conditional generation on the additional image-grounded guidance acts as a controllable gate. Only objects with relatively high probabilities in both branches could appear at top when sampling. Specifically, setting  $\gamma = 0$  recovers the original LLM generation without control guidance and setting  $\gamma = 1$  produces the LLM generation entirely based on the control. Meanwhile, for  $\gamma \in (0, 1)$ , MARINE yields a combination of the original generation  $p_\theta(\mathbf{y}|\mathbf{v}, \mathbf{x})$  and the generation conditioned on the guidance  $p_\theta(\mathbf{y}|\mathbf{v}, \mathbf{c}, \mathbf{x})$ . This strikes a balance between a better ability to follow instructions to generate high-quality answers and the increased accuracy and detail in image descriptions. The formulation therefore shares resemblance to the classifier-free guidance introduced for LLMs (Sanchez et al., 2023), which places importance on the textual prompt itself to better align the LLM generation with user intention in the *single-modal* setting. We summarize MARINE in Algorithm 1. In detail, MARINE aggregates the collected visual information  $\{\mathbf{c}_i\}_i$  using function Aggr., which can be a small language model for information aggregation (Lin et al., 2023a), or a rule-based algorithms like majority voting (as similarly used by Wang et al.). Notably, MARINE only double the LLM inference time of in Line 7 and Line 9, while adding the guidance from each single image grounded model will increase the inference time when the number of image grounded models increase.

## 5 EXPERIMENTS

In this section, we evaluate MARINE in mitigating object hallucinations across various LVLms, showing that it outperforms state-of-the-art methods on established metrics across different datasets.

### 5.1 EXPERIMENT SETUP

**Models.** To demonstrate the broad applicability of our approach across different LVLm architectures, we apply and evaluate MARINE to recent widely-used models including *LLaVA* (Liu et al., 2023d), *LLaVA-v1.5* (Liu et al., 2023c), *MiniGPT-v2* (Chen et al., 2023), *mPLUG-Owl2* (Ye et al., 2023) and *InstructBLIP* (Liu et al., 2023c). To address the object hallucination problems in text generation, we incorporate the DETection TRansformer (DETR) (Carion et al., 2020) and RAM++ (Huang et al., 2023b) as the additional vision models for guidance.

**Guidance from Multiple Sources.** Our framework’s compatibility with various vision models allows for the incorporation of multiple sources to enhance precision and robustness. By considering object-level information from DETR and RAM++ simultaneously, we generate guidance that reflects

---

**Algorithm 1** Mitigating hallucination via image-gRounded guIdaNcE (MARINE)

- 1: **Input:** LLM parameter  $\theta$ , input prompt  $\mathbf{x}$ , visual tokens  $\mathbf{v}$  from LVLM’s original vision tower
  - 2: **Input:** auxiliary visual tokens  $\{\mathbf{c}_i\}_{i=1}^M$  from  $M$  image grounding models, guidance scale  $\gamma$
  - 3: Initialize empty output  $\mathbf{y} = []$ .
  - 4: Aggregate visual information as textual prompt  $\mathbf{c} = \text{Aggr.}(\{\mathbf{c}_i\}_{i=1}^M)$
  - 5: **for**  $t = 0, 1, \dots, T$  **do**
  - 6:   Construct unconditional input  $\mathbf{x}_{\text{uncond}}^{(t)} = [\mathbf{v}, \mathbf{x}, \mathbf{y}_{<t}]$ .
  - 7:   Generate unconditional output logits using LLM:  $\ell_{\text{uncond}}^{(t)} = \log p_{\theta}(\mathbf{x}_{\text{uncond}}^{(t)})$ .
  - 8:   Construct conditional input  $\mathbf{x}_{\text{cond}}^{(t)} = [\mathbf{v}, \mathbf{c}, \mathbf{x}, \mathbf{y}_{<t}]$ .
  - 9:   Generate conditional output logits using LLM:  $\ell_{\text{cond}}^{(t)} = \log p_{\theta}(\mathbf{x}_{\text{cond}}^{(t)})$ .
  - 10:   Update output logits  $\ell^{(t)} = \gamma \ell_{\text{cond}}^{(t)} + (1 - \gamma) \ell_{\text{uncond}}^{(t)}$ .
  - 11:   Sample token  $y_t$  from logit space denoted by  $\ell^{(t)}$ .
  - 12:   Let  $\mathbf{y} = [\mathbf{y}, y_t]$ .
  - 13: **end for**
  - 14: **Output:**  $\mathbf{y}$ .
- 

consensus across these models. This approach significantly improves the accuracy and reliability of the guidance provided to the LVLM.

**Datasets and evaluations.** In alignment with established evaluations from previous studies (Dai et al., 2023b; Yin et al., 2023), we assess our method using the following metrics:

- Caption Hallucination Assessment with Image Relevance (CHAIR) (Rohrbach et al., 2018). It involves prompting the LVLMs to generate a description for the input image, and then comparing this generation with ground truth objects present in the image. CHAIR quantifies hallucination both at instance level and sentence level, respectively defined as  $\text{CHAIR}_I$  and  $\text{CHAIR}_S$ :

$$\text{CHAIR}_I = \frac{|\{\text{hallucinated objects}\}|}{|\{\text{all mentioned objects}\}|}, \quad \text{CHAIR}_S = \frac{|\{\text{captions with hallucinated objects}\}|}{|\{\text{all captions}\}|}.$$

In addition to these metrics, we incorporate an instance-level Recall score in our evaluation to evaluate whether the descriptions accurately include the necessary visual content from the image:

$$\text{Recall} = \frac{|\{\text{non-hallucinated objects}\}|}{|\{\text{all existing objects}\}|}.$$

- Polling-based Object Probing Evaluation (POPE) (Li et al., 2023b). POPE formulates a binary classification task by prompting LVLMs with questions such as “Is there a keyboard in this image?” to answer “yes” or “no”. We specifically focus on the adversarial setting, which is considered the most challenging setting. Results for the random and popular settings are detailed in Appendix E. We report the accuracy and F1 score of the LVLMs’ responses, and the proportion of “yes” answers.
- GPT-4V-aided Evaluation (Yin et al., 2023). The GPT-4V-aided evaluation compares the outputs of two LVLM assistants using GPT-4V as a judge. In this evaluation, we utilize the LLaVA-QA90 task (Liu et al., 2023d)\* (including conversations, visual perceptions, and complex reasoning tasks) and additionally consider the image captioning task.

Consistent with Li et al. (2023b), we randomly sampled a subset of 500 images from MSCOCO (Lin et al., 2014) dataset for CHAIR evaluation. For the POPE evaluation, we created 3000 questions across three datasets—500 images each from MSCOCO, A-OKVQA (Schwenk et al., 2022), and GQA (Hudson & Manning, 2019). For the GPT-4V-aided evaluation, we utilized 90 questions from the LLaVA-QA90 task and randomly selected 50 MSCOCO images for image captioning task. We defer the detailed description of our baselines to Appendix D.

## 5.2 RESULTS

Experimental results on object hallucination metrics (CHAIR and POPE) are presented in Table 1 and Table 2. Overall, MARINE achieves superior performances across different LVLM architectures and evaluation metrics, ranked as the best or second-best on the majority of the evaluation metrics.

**Results on CHAIR.** Table 1 presents the evaluation of various mitigation methods using CHAIR scores across multiple LVLM architectures. The results demonstrate that MARINE consistently outperforms other state-of-the-art methods, achieving the highest average scores in both  $\text{CHAIR}_I$  and  $\text{CHAIR}_S$  and

---

\*[https://github.com/haotian-liu/LLaVA/blob/main/playground/data/coco2014\\_val\\_gpt4\\_qa\\_30x3.jsonl](https://github.com/haotian-liu/LLaVA/blob/main/playground/data/coco2014_val_gpt4_qa_30x3.jsonl)

Table 1: Evaluation with CHAIR score across multiple LVLM architectures comparing our method with several baselines. We report CHAIR<sub>S</sub>, CHAIR<sub>I</sub> and the recall score. The **bold** numbers indicate the best results among the methods evaluated and the underscored numbers represent the second-best results. We show MARINE-Truth as a reference performance of MARINE.

Method	LLaVA			LLaVA-v1.5			MiniGPTv2			mPLUG-Owl2			InstructBLIP			Average		
	C <sub>S</sub> ↓	C <sub>I</sub> ↓	R ↑	C <sub>S</sub> ↓	C <sub>I</sub> ↓	R ↑	C <sub>S</sub> ↓	C <sub>I</sub> ↓	R ↑	C <sub>S</sub> ↓	C <sub>I</sub> ↓	R ↑	C <sub>S</sub> ↓	C <sub>I</sub> ↓	R ↑	C <sub>S</sub> ↓	C <sub>I</sub> ↓	R ↑
<b>CHAIR</b>	C <sub>S</sub> ↓	C <sub>I</sub> ↓	R ↑	C <sub>S</sub> ↓	C <sub>I</sub> ↓	R ↑	C <sub>S</sub> ↓	C <sub>I</sub> ↓	R ↑	C <sub>S</sub> ↓	C <sub>I</sub> ↓	R ↑	C <sub>S</sub> ↓	C <sub>I</sub> ↓	R ↑	C <sub>S</sub> ↓	C <sub>I</sub> ↓	R ↑
Greedy	26.6	10.5	47.4	8.8	4.6	41.1	8.2	<u>4.2</u>	41.1	6.2	3.4	38.8	5.0	3.2	33.2	11.0	5.2	40.3
LURE	33.8	11.6	<b>54.8</b>	38.9	11.2	<b>56.3</b>	36.2	11.4	<b>54.6</b>	33.9	10.8	<b>55.9</b>	38.1	12.1	<b>54.5</b>	36.2	11.4	<b>55.2</b>
LURE w/ cutoff	24.4	9.3	50.2	18.4	6.8	<u>47.3</u>	12.5	6.2	42.0	15.4	6.6	<u>45.5</u>	9.6	6.4	34.5	16.1	7.1	43.9
Woodpecker	19.5	<u>8.9</u>	44.3	8.5	4.5	38.4	<u>7.5</u>	4.5	37.0	8.0	4.3	37.5	8.0	6.2	32.6	10.3	5.7	38.0
VCD	28.1	11.0	46.6	<u>7.3</u>	<u>4.1</u>	40.8	<b>6.8</b>	<b>3.9</b>	38.2	<u>5.9</u>	3.4	37.7	<u>2.4</u>	<u>1.5</u>	33.7	<u>10.1</u>	<u>4.8</u>	39.4
OPERA	<u>22.4</u>	9.9	43.6	11.0	6.7	40.2	9.2	5.0	41.3	5.8	<u>3.2</u>	38.4	4.6	2.7	<u>38.0</u>	10.6	5.5	40.3
<b>MARINE</b>	<b>17.8</b>	<b>7.2</b>	<u>50.8</u>	<b>6.2</b>	<b>3.0</b>	44.3	11.8	4.9	<u>49.7</u>	<b>4.2</b>	<b>2.3</b>	41.4	<b>2.2</b>	<b>1.3</b>	36.3	<b>8.4</b>	<b>3.7</b>	<u>44.5</u>
MARINE-Truth	19.6	5.1	12.6	6.0	2.5	55.3	12.6	3.8	2.7	3.8	1.7	48.0	3.0	1.8	35.9	9.0	3.0	30.9

Table 2: Evaluation with POPE score in adversarial setting across multiple LVLM architectures comparing our method with several baselines. We report the POPE accuracy (%), F1 score (%) and the yes ratio (%). The ideal yes ratio for a non-biased LVLM is 50%. The **bold** numbers indicate the best results among the methods evaluated and the underscored numbers represent the second-best results. We show MARINE-Truth as a reference performance of MARINE.

Method	LLaVA			LLaVA-v1.5			MiniGPTv2			mPLUG-Owl2			InstructBLIP			Average		
	Acc ↑	F1 ↑	Yes	Acc ↑	F1 ↑	Yes	Acc ↑	F1 ↑	Yes	Acc ↑	F1 ↑	Yes	Acc ↑	F1 ↑	Yes	Acc ↑	F1 ↑	Yes
Greedy	51.8	67.4	97.7	79.4	<u>81.6</u>	61.6	82.7	81.7	<u>44.5</u>	72.5	77.5	72.4	<u>79.8</u>	<b>81.4</b>	58.6	73.2	77.9	67.0
LURE	-	-	-	-	-	-	-	-	-	-	-	-	-	-	-	-	-	-
Woodpecker	<b>77.5</b>	<b>77.6</b>	<b>50.5</b>	80.5	80.6	<b>50.5</b>	79.5	77.8	42.5	77.5	76.9	<u>47.5</u>	79.0	78.6	<b>48.0</b>	<u>78.8</u>	<u>78.3</u>	<u>47.8</u>
VCD	54.6	68.5	94.0	78.2	80.7	62.8	81.4	80.2	44.1	72.3	77.0	70.5	79.7	<u>80.9</u>	<u>56.7</u>	73.2	77.5	65.6
OPERA	51.7	67.4	98.0	77.5	80.1	63.2	<u>82.9</u>	<u>81.9</u>	44.3	70.3	<u>79.1</u>	84.6	<u>79.8</u>	<b>81.4</b>	58.6	72.4	78.0	69.7
<b>MARINE</b>	<u>66.9</u>	<u>72.9</u>	<u>72.3</u>	<b>85.0</b>	<b>84.3</b>	<u>45.7</u>	<b>83.0</b>	<b>82.9</b>	<b>49.4</b>	<b>82.8</b>	<b>82.7</b>	<b>49.2</b>	<b>81.7</b>	79.4	38.8	<b>79.9</b>	<b>80.4</b>	<b>51.1</b>
MARINE-Truth	75.6	72.3	80.1	92.0	57.0	92.5	86.9	62.5	88.3	77.5	72.1	81.6	93.8	51.0	93.8	85.2	63.0	87.3

CHAIR<sub>I</sub> and the second-best Recall score. Specifically, MARINE surpasses the second-best performing method by an average margin of 1.7 on CHAIR<sub>S</sub> and 1.1 on CHAIR<sub>I</sub>. Notably, MARINE exhibits exceptional performance on LLaVA architectures, with improvements in CHAIR scores of up to 8.8 compared to its original performance. In contrast, methods such as LURE and Woodpecker show less effectiveness in hallucination mitigation. The reference method, MARINE-Truth, generally achieves the strongest results, as expected given its access to ground-truth guidance. However, MARINE’s performance closely approximates that of its ground-truth counterpart, indicating successful leveraging of multiple guidance models to provide reliable control in LVLM generation.

**Results on POPE.** The POPE evaluation, presented in Table 2, further validates the superior performance of MARINE against existing baselines across various question formats. MARINE consistently outperforms all other methods by a substantial margin, demonstrating average improvements of 6.7% in accuracy and 3.5% in F1 score relative to the original outputs across models. Even when compared to the second-best method, Woodpecker, MARINE maintains a performance edge of 1.1% and 2.1% respectively in accuracy and F1 score. Moreover, MARINE effectively mitigates the LVLMs’ biased tendency towards affirmative responses, as evidenced by a more balanced "yes" ratio (closer to 50%, representing a 15.9% shift towards unbiased answers). This improvement notably addresses the overconfidence issue prevalent in existing models.

**Results on GPT-4V-aided evaluation.** Following Yin et al. (2023), we leverage GPT-4V\* to evaluate and compare the performance of the original LVLMs and LVLMs with MARINE on LLaVA-QA90 and an image captioning task. This GPT-4V-assisted evaluation introduces a qualitative perspective beyond the numerical metrics of CHAIR and POPE, offering a richer assessment of model performance. The evaluation prompt is detailed in Appendix D.6. As shown in Table 3, GPT-4V consistently assigns higher accuracy with equal detailedness scores to models enhanced by MARINE, highlighting its ability to produce more precise and detailed descriptions, which demonstrates the robustness of our method in real-world visual tasks.

**Additional Results on Other Vision-Language Tasks.** To further evaluate the generalizability of our approach beyond object hallucination and the MSCOCO dataset, we extended our evaluations to additional datasets including A-OKVQA and GQA and included more general caption quality metrics. As shown in Table 4, the POPE results on datasets such as MSCOCO, A-OKVQA, and

\*We used gpt-4-1106-vision-preview in obtaining our final experiment results. As OpenAI continues to update its API, different versions may result in slightly different values.

Table 3: Results of GPT-4V-aided evaluation. The accuracy and detailedness metrics are on a scale of 10, and a higher score indicates better performance. The symbols  $\times$  and  $\checkmark$  indicate performance metrics without and with our method, respectively.

Task	Metrics	LLaVA		mPLUG-Owl2	
		$\times$	$\checkmark$	$\times$	$\checkmark$
LLaVA-QA90	Acc $\uparrow$	5.82 $\pm$ 0.10	<b>5.94</b> $\pm$ 0.05	6.03 $\pm$ 0.13	<b>6.35</b> $\pm$ 0.21
	Detail $\uparrow$	4.59 $\pm$ 0.08	4.59 $\pm$ 0.08	5.06 $\pm$ 0.05	<b>5.16</b> $\pm$ 0.10
Image Captioning	Acc $\uparrow$	5.27 $\pm$ 0.20	<b>6.11</b> $\pm$ 0.23	7.97 $\pm$ 0.25	<b>8.63</b> $\pm$ 0.20
	Detail $\uparrow$	<b>4.39</b> $\pm$ 0.29	4.36 $\pm$ 0.17	5.74 $\pm$ 0.24	<b>6.19</b> $\pm$ 0.23

Table 4: POPE results across three datasets. We report the average score under random, popular, adversarial settings. The detailed POPE results can be found in the appendix E. The **bold** numbers indicate the best results. The ideal yes ratio for a non-biased LVLm is 50%.

Dataset	w/MARINE	LLaVA			mPLUG-Owl2		
		Accuracy $\uparrow$	F1 $\uparrow$	Yes(%)	Accuracy $\uparrow$	F1 $\uparrow$	Yes(%)
MSCOCO (Lin et al., 2014)	$\times$	54.2	68.5	95.5	76.7	80.4	68.2
	$\checkmark$	<b>72.2</b>	<b>76.4</b>	<b>66.9</b>	<b>85.5</b>	<b>85.0</b>	<b>46.5</b>
A-OKVQA (Schwenk et al., 2022)	$\times$	51.8	67.5	97.9	69.6	76.5	78.5
	$\checkmark$	<b>64.3</b>	<b>72.8</b>	<b>80.2</b>	<b>82.0</b>	<b>83.5</b>	<b>57.2</b>
GQA (Hudson & Manning, 2019)	$\times$	52.0	67.6	97.8	73.7	78.7	72.6
	$\checkmark$	<b>62.5</b>	<b>71.8</b>	<b>81.8</b>	<b>80.1</b>	<b>80.6</b>	<b>51.1</b>

GQA demonstrate that our method consistently mitigates hallucinations across various datasets with different image distributions. Figure 2 presents a comprehensive evaluation of the image captioning task on MSCOCO and LLaVA-QA90, a comprehensive VQA dataset, using metrics including BLEU (Papineni et al., 2002), ROUGE (Lin, 2004), CIDEr (Vedantam et al., 2015) and SPICE (Anderson et al., 2016). These results demonstrate that, although our method primarily targets hallucination mitigation, it maintains the overall performance of LVLms on broader tasks, with no significant trade-offs in caption or VQA quality.

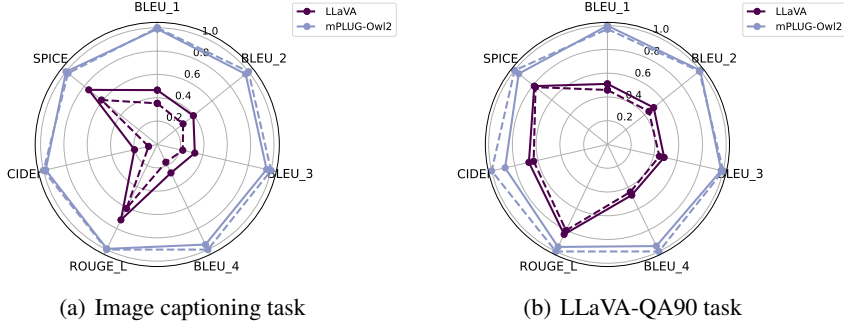


Figure 2: MARINE leads to consistent enhancement in the text qualities on general metrics. Dashed lines and solid lines represent without or with MARINE. Higher scores indicate better quality and greater similarity between the generated captions and the reference texts.

**Latency Analysis** Mitigating object hallucination often requires additional computational resources, a characteristic common to many existing methods which typically involve additional post-generation correction models (Zhou et al., 2023; Zhai et al., 2023; Yin et al., 2023), object detectors (Yin et al., 2023), or more complex decoding processes (Huang et al., 2023a; Leng et al., 2023) to reduce hallucinations. Furthermore, to assess the practical feasibility of our approach in terms of computational costs, we have compared our method with existing baselines on LLaVA-7B. As demonstrated in Table 5, our method increases the decoding time by factors of 1.98, which is the lowest costs among existing baselines, suggesting MARINE can be widely applied with negligible cost. Our method offers the most favorable trade-offs between latency and accuracy in hallucination mitigation. Detailed experiment setting is in Appendix D.7.

### 5.3 ABLATION STUDY

**How Does Incorporating Multiple Sources to Form Guidance Impact Performance?** We perform an ablation study to assess the impact of incorporating DETR and RAM++ compared to using each model individually, as presented in Table 6. Notably, DETR allows for highly accurate object detection, while RAM++ excels in extensive recognition tasks, adding fine-grained details to image

Table 5: Inference Latency Comparison. We report both the latency and the ratio to the latency of greedy decoding of the original LVLm model.

	Greedy	LURE	Woodpecker*	VCD	OPERA	MARINE (ours)
Training Cost	0	10min on A100 80G	0	0	0	0
Inference Latency <sup>(ms/token)</sup>	26.3 (×1.0)	179.9 (×6.84)	94.5 (×3.59)*	53.4 (×2.03)	185.1 (×7.0)	<b>52.2 (×1.98)</b>

\*Woodpecker requires GPT API key access and the latency may depend on OPENAI API.

Table 6: Ablation study comparing the performance of combining DETR and RAM++ models versus using individual vision models. This approach leverages multiple object detectors to provide more reliable and robust object-level guidance, resulting in superior performance on CHAIR metrics.

Model	LLaVA		LLaVA-v1.5		mPLUG-Owl2	
	$C_S \downarrow$	$C_I \downarrow$	$C_S \downarrow$	$C_I \downarrow$	$C_S \downarrow$	$C_I \downarrow$
<i>Ensembling Models</i>						
MARINE	<b>17.8</b>	<b>7.2</b>	<b>6.2</b>	<b>3.0</b>	<b>4.2</b>	<b>2.3</b>
<i>Single Models</i>						
MARINE-DETR only	27.6	8.4	10.5	4.3	5.3	2.7
MARINE-RAM only	29.0	9.1	6.6	3.7	5.2	2.8

Table 7: Effect of Integration Methods for Image-Grounding Models.

Model	LLaVA		LLaVA-v1.5		mPLUG-Owl2	
	$C_S \downarrow$	$C_I \downarrow$	$C_S \downarrow$	$C_I \downarrow$	$C_S \downarrow$	$C_I \downarrow$
MARINE-intersection (ours)	<b>17.8</b>	<b>7.2</b>	<b>6.2</b>	<b>3.0</b>	<b>4.2</b>	<b>2.3</b>
MARINE-union	30.4	9.7	5.4	2.7	4.8	2.7

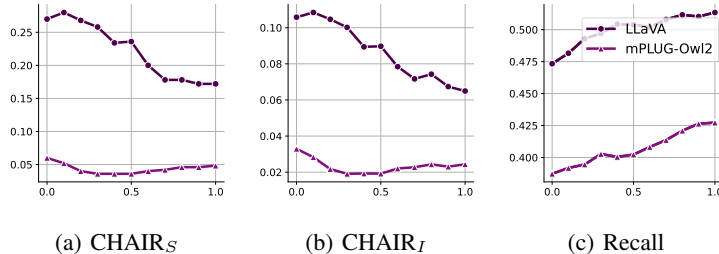


Figure 3: Ablation study on the effect of guidance strength ( $\gamma$ ) on the performance of LLaVA and mPLUG-Owl2 using CHAIR metrics, with  $\gamma$  ranging from 0 to 1.

understanding. Combining the strengths of these image-grounding models, we achieve significant performance improvements on the CHAIR metrics. This demonstrates that leveraging complementary visual contexts can substantially enhance overall model effectiveness.

**Which Method of Integrating Image-Grounding Models Works Best?** We investigate two approaches for integrating image-grounding models: using either the intersection or union of detected objects. As shown in Table 7, the intersection-based method outperforms the union, significantly reducing object hallucination. This result highlights the importance of precision and consistency in guidance, as taking intersection ensures consensus across models, leading to more reliable guidance. The detailed experimental setup and prompt templates are provided in Appendix D.

**Effect of Guidance Strength.** Figure 3 shows that increasing guidance strength from 0 to 1 leads to a notable decrease in CHAIR scores. This trend suggests that higher guidance strength makes LVLmS rely more on image-grounded features provided by the guidance models, thereby enhancing their ability to produce accurate descriptions. It’s crucial to note that, although some models exhibit optimal performance at a guidance strength of  $\gamma = 1$ , excessively strong guidance can adversely affect the models’ ability to adhere to provided instructions. Experimental evidence is detailed in Appendix E. Based on our findings, we recommend a guidance strength within the range of  $\gamma \in (0.3, 0.7)$  as the most effective for maintaining this balance.

## 6 CONCLUSION

In this paper, we introduced a training-free and API-free framework MARINE to mitigate object hallucination in LVLmS during its text generation process. Leveraging a pre-trained object grounding vision encoder for a novel guidance framework in the multi-modal setting, MARINE effectively



---

and cost-efficiently reduces the hallucinations of five widely-used LVLMs, as assessed by various metrics across different tasks. The inherent compatibility of the MARINE with various vision models and projection functions further underscores its flexibility. In contrast to post-generation correction methods, MARINE strikes a balance between efficiency, instruction-following ability and effectiveness in reducing object hallucinations.

---

## REFERENCES

- Jean-Baptiste Alayrac, Jeff Donahue, Pauline Luc, Antoine Miech, Iain Barr, Yana Hasson, Karel Lenc, Arthur Mensch, Katherine Millican, Malcolm Reynolds, et al. Flamingo: a visual language model for few-shot learning. *Advances in Neural Information Processing Systems*, 35:23716–23736, 2022. [1](#)
- Peter Anderson, Basura Fernando, Mark Johnson, and Stephen Gould. Spice: Semantic propositional image caption evaluation, 2016. [7](#), [16](#), [21](#)
- Yakoub Bazi, Mohamad Mahmoud Al Rahhal, Laila Bashmal, and Mansour Zuair. Vision–language model for visual question answering in medical imagery. *Bioengineering*, 10(3):380, 2023. [1](#)
- Steven Bird, Ewan Klein, and Edward Loper. *Natural language processing with Python: analyzing text with the natural language toolkit*. " O’Reilly Media, Inc.", 2009. [4](#)
- Ali Furkan Biten, Lluís Gómez, and Dimosthenis Karatzas. Let there be a clock on the beach: Reducing object hallucination in image captioning. In *Proceedings of the IEEE/CVF Winter Conference on Applications of Computer Vision*, pp. 1381–1390, 2022. [3](#)
- Nicolas Carion, Francisco Massa, Gabriel Synnaeve, Nicolas Usunier, Alexander Kirillov, and Sergey Zagoruyko. End-to-end object detection with transformers. In *European conference on computer vision*, pp. 213–229. Springer, 2020. [2](#), [4](#)
- Fredrik Carlsson, Joey Öhman, Fangyu Liu, Severine Verlinden, Joakim Nivre, and Magnus Sahlgren. Fine-grained controllable text generation using non-residual prompting. In *Proceedings of the 60th Annual Meeting of the Association for Computational Linguistics (Volume 1: Long Papers)*, pp. 6837–6857, 2022. [15](#)
- Pierre Chambon, Christian Bluethgen, Curtis P Langlotz, and Akshay Chaudhari. Adapting pretrained vision-language foundational models to medical imaging domains. *arXiv preprint arXiv:2210.04133*, 2022. [1](#)
- Jun Chen, Deyao Zhu, Xiaoqian Shen, Xiang Li, Zechun Liu, Pengchuan Zhang, Raghuraman Krishnamoorthi, Vikas Chandra, Yunyang Xiong, and Mohamed Elhoseiny. Minigt-v2: large language model as a unified interface for vision-language multi-task learning. *arXiv preprint arXiv:2310.09478*, 2023. [4](#), [16](#)
- Zhaorun Chen, Zhuokai Zhao, Hongyin Luo, Huaxiu Yao, Bo Li, and Jiawei Zhou. Halc: Object hallucination reduction via adaptive focal-contrast decoding. *arXiv preprint arXiv:2403.00425*, 2024. [3](#)
- Wei-Lin Chiang, Zhuohan Li, Zi Lin, Ying Sheng, Zhanghao Wu, Hao Zhang, Lianmin Zheng, Siyuan Zhuang, Yonghao Zhuang, Joseph E. Gonzalez, Ion Stoica, and Eric P. Xing. Vicuna: An open-source chatbot impressing gpt-4 with 90%\* chatgpt quality, March 2023. [16](#)
- Wenliang Dai, Junnan Li, Dongxu Li, Anthony Meng Huat Tiong, Junqi Zhao, Weisheng Wang, Boyang Li, Pascale Fung, and Steven Hoi. Instructblip: Towards general-purpose vision-language models with instruction tuning, 2023a. [1](#), [3](#), [16](#)
- Wenliang Dai, Zihan Liu, Ziwei Ji, Dan Su, and Pascale Fung. Plausible may not be faithful: Probing object hallucination in vision-language pre-training. In *Proceedings of the 17th Conference of the European Chapter of the Association for Computational Linguistics*, pp. 2128–2140, 2023b. [3](#), [5](#)
- Yihe Deng, Pan Lu, Fan Yin, Ziniu Hu, Sheng Shen, James Zou, Kai-Wei Chang, and Wei Wang. Enhancing large vision language models with self-training on image comprehension. *arXiv preprint arXiv:2405.19716*, 2024. [1](#)
- Prafulla Dhariwal and Alexander Nichol. Diffusion models beat gans on image synthesis. *Advances in neural information processing systems*, 34:8780–8794, 2021. [15](#)
- Alexey Dosovitskiy, Lucas Beyer, Alexander Kolesnikov, Dirk Weissenborn, Xiaohua Zhai, Thomas Unterthiner, Mostafa Dehghani, Matthias Minderer, Georg Heigold, Sylvain Gelly, et al. An image is worth 16x16 words: Transformers for image recognition at scale. *arXiv preprint arXiv:2010.11929*, 2020. [16](#)

- 
- Yuxin Fang, Wen Wang, Binhui Xie, Quan Sun, Ledell Wu, Xinggang Wang, Tiejun Huang, Xinlong Wang, and Yue Cao. Eva: Exploring the limits of masked visual representation learning at scale. In *Proceedings of the IEEE/CVF Conference on Computer Vision and Pattern Recognition*, pp. 19358–19369, 2023. 16
- Chaoyou Fu, Peixian Chen, Yunhang Shen, Yulei Qin, Mengdan Zhang, Xu Lin, Zhenyu Qiu, Wei Lin, Jinrui Yang, Xiawu Zheng, et al. Mme: A comprehensive evaluation benchmark for multimodal large language models. *arXiv preprint arXiv:2306.13394*, 2023. 1, 3
- Peng Gao, Jiaming Han, Renrui Zhang, Ziyi Lin, Shijie Geng, Aojun Zhou, Wei Zhang, Pan Lu, Conghui He, Xiangyu Yue, Hongsheng Li, and Yu Qiao. Llama-adapter v2: Parameter-efficient visual instruction model, 2023. 1, 3
- Anisha Gunjal, Jihan Yin, and Erhan Bas. Detecting and preventing hallucinations in large vision language models. *arXiv preprint arXiv:2308.06394*, 2023. 1, 3
- Jonathan Ho and Tim Salimans. Classifier-free diffusion guidance. In *NeurIPS 2021 Workshop on Deep Generative Models and Downstream Applications*, 2021. 15
- Zhiting Hu and Li Erran Li. A causal lens for controllable text generation. *Advances in Neural Information Processing Systems*, 34:24941–24955, 2021. 15
- Qidong Huang, Xiaoyi Dong, Pan Zhang, Bin Wang, Conghui He, Jiaqi Wang, Dahua Lin, Weiming Zhang, and Nenghai Yu. Opera: Alleviating hallucination in multi-modal large language models via over-trust penalty and retrospection-allocation. *arXiv preprint arXiv:2311.17911*, 2023a. 3, 7, 15, 17
- Xinyu Huang, Yi-Jie Huang, Youcai Zhang, Weiwei Tian, Rui Feng, Yuejie Zhang, Yanchun Xie, Yaqian Li, and Lei Zhang. Open-set image tagging with multi-grained text supervision, 2023b. URL <https://arxiv.org/abs/2310.15200>. 2, 4
- Drew A Hudson and Christopher D Manning. Gqa: A new dataset for real-world visual reasoning and compositional question answering. In *Proceedings of the IEEE/CVF conference on computer vision and pattern recognition*, pp. 6700–6709, 2019. 2, 5, 7, 20
- Ziwei Ji, Nayeon Lee, Rita Frieske, Tiezheng Yu, Dan Su, Yan Xu, Etsuko Ishii, Ye Jin Bang, Andrea Madotto, and Pascale Fung. Survey of hallucination in natural language generation. *ACM Computing Surveys*, 55(12):1–38, 2023. 1
- Chao Jia, Yinfei Yang, Ye Xia, Yi-Ting Chen, Zarana Parekh, Hieu Pham, Quoc Le, Yun-Hsuan Sung, Zhen Li, and Tom Duerig. Scaling up visual and vision-language representation learning with noisy text supervision. In *International Conference on Machine Learning*, pp. 4904–4916. PMLR, 2021. 1
- Liqiang Jing, Ruosen Li, Yunmo Chen, Mengzhao Jia, and Xinya Du. Faithscore: Evaluating hallucinations in large vision-language models. *arXiv preprint arXiv:2311.01477*, 2023. 1
- Sicong Leng, Hang Zhang, Guanzheng Chen, Xin Li, Shijian Lu, Chunyan Miao, and Lidong Bing. Mitigating object hallucinations in large vision-language models through visual contrastive decoding. *arXiv preprint arXiv:2311.16922*, 2023. 3, 7, 15, 17
- Junnan Li, Dongxu Li, Silvio Savarese, and Steven Hoi. Blip-2: Bootstrapping language-image pre-training with frozen image encoders and large language models. *arXiv preprint arXiv:2301.12597*, 2023a. 16
- Xiang Li, John Thickstun, Ishaan Gulrajani, Percy S Liang, and Tatsunori B Hashimoto. Diffusion-lm improves controllable text generation. *Advances in Neural Information Processing Systems*, 35: 4328–4343, 2022. 15
- Xiang Lisa Li and Percy Liang. Prefix-tuning: Optimizing continuous prompts for generation. In *Proceedings of the 59th Annual Meeting of the Association for Computational Linguistics and the 11th International Joint Conference on Natural Language Processing (Volume 1: Long Papers)*, pp. 4582–4597, 2021. 15

- 
- Yifan Li, Yifan Du, Kun Zhou, Jinpeng Wang, Wayne Xin Zhao, and Ji-Rong Wen. Evaluating object hallucination in large vision-language models. *arXiv preprint arXiv:2305.10355*, 2023b. [1](#), [2](#), [3](#), [5](#), [17](#), [18](#), [20](#)
- Chin-Yew Lin. ROUGE: A package for automatic evaluation of summaries. In *Text Summarization Branches Out*, pp. 74–81, Barcelona, Spain, July 2004. Association for Computational Linguistics. URL <https://aclanthology.org/W04-1013>. [7](#), [16](#), [21](#)
- Sheng-Chieh Lin, Minghan Li, and Jimmy Lin. Aggretriever: A simple approach to aggregate textual representations for robust dense passage retrieval. *Transactions of the Association for Computational Linguistics*, 11:436–452, 2023a. [4](#)
- Tsung-Yi Lin, Michael Maire, Serge Belongie, James Hays, Pietro Perona, Deva Ramanan, Piotr Dollár, and C Lawrence Zitnick. Microsoft coco: Common objects in context. In *Computer Vision—ECCV 2014: 13th European Conference, Zurich, Switzerland, September 6-12, 2014, Proceedings, Part V 13*, pp. 740–755. Springer, 2014. [2](#), [5](#), [7](#), [20](#)
- Zhaojiang Lin, Andrea Madotto, Yejin Bang, and Pascale Fung. The adapter-bot: All-in-one controllable conversational model. In *Proceedings of the AAAI Conference on Artificial Intelligence*, volume 35, pp. 16081–16083, 2021. [15](#)
- Zhenghao Lin, Yeyun Gong, Yelong Shen, Tong Wu, Zhihao Fan, Chen Lin, Nan Duan, and Weizhu Chen. Text generation with diffusion language models: A pre-training approach with continuous paragraph denoise. In *International Conference on Machine Learning*, pp. 21051–21064. PMLR, 2023b. [15](#)
- Fuxiao Liu, Kevin Lin, Linjie Li, Jianfeng Wang, Yaser Yacoob, and Lijuan Wang. Aligning large multi-modal model with robust instruction tuning. *arXiv preprint arXiv:2306.14565*, 2023a. [1](#)
- Fuxiao Liu, Kevin Lin, Linjie Li, Jianfeng Wang, Yaser Yacoob, and Lijuan Wang. Mitigating hallucination in large multi-modal models via robust instruction tuning, 2023b. [1](#), [3](#)
- Haotian Liu, Chunyuan Li, Yuheng Li, and Yong Jae Lee. Improved baselines with visual instruction tuning. *arXiv preprint arXiv:2310.03744*, 2023c. [4](#), [16](#)
- Haotian Liu, Chunyuan Li, Qingyang Wu, and Yong Jae Lee. Visual instruction tuning. In *NeurIPS*, 2023d. [1](#), [2](#), [3](#), [4](#), [5](#), [16](#), [20](#)
- Holy Lovenia, Wenliang Dai, Samuel Cahyawijaya, Ziwei Ji, and Pascale Fung. Negative object presence evaluation (nope) to measure object hallucination in vision-language models. *arXiv preprint arXiv:2310.05338*, 2023. [1](#), [3](#)
- Jiasen Lu, Jianwei Yang, Dhruv Batra, and Devi Parikh. Neural baby talk. In *2018 IEEE/CVF Conference on Computer Vision and Pattern Recognition*, pp. 7219–7228, 2018. doi: 10.1109/CVPR.2018.00754. [17](#)
- Pan Lu, Hritik Bansal, Tony Xia, Jiacheng Liu, Chunyuan Li, Hannaneh Hajishirzi, Hao Cheng, Kai-Wei Chang, Michel Galley, and Jianfeng Gao. Mathvista: Evaluating mathematical reasoning of foundation models in visual contexts, 2024. [1](#)
- Aman Madaan, Amrith Setlur, Tanmay Parekh, Barnabás Póczós, Graham Neubig, Yiming Yang, Ruslan Salakhutdinov, Alan W Black, and Shrimai Prabhunoye. Politeness transfer: A tag and generate approach. In *Proceedings of the 58th Annual Meeting of the Association for Computational Linguistics*, pp. 1869–1881, 2020. [15](#)
- Tong Niu and Mohit Bansal. Polite dialogue generation without parallel data. *Transactions of the Association for Computational Linguistics*, 6:373–389, 2018. [15](#)
- Long Ouyang, Jeffrey Wu, Xu Jiang, Diogo Almeida, Carroll Wainwright, Pamela Mishkin, Chong Zhang, Sandhini Agarwal, Katarina Slama, Alex Ray, et al. Training language models to follow instructions with human feedback. *Advances in Neural Information Processing Systems*, 35: 27730–27744, 2022. [15](#)

- 
- Kishore Papineni, Salim Roukos, Todd Ward, and Wei-Jing Zhu. Bleu: a method for automatic evaluation of machine translation. In *Proceedings of the 40th annual meeting of the Association for Computational Linguistics*, pp. 311–318, 2002. [7](#), [16](#), [21](#)
- Shrimai Prabhunoye, Alan W Black, and Ruslan Salakhutdinov. Exploring controllable text generation techniques. In *Proceedings of the 28th International Conference on Computational Linguistics*, pp. 1–14, 2020. [15](#)
- Alec Radford, Jong Wook Kim, Chris Hallacy, Aditya Ramesh, Gabriel Goh, Sandhini Agarwal, Girish Sastry, Amanda Askell, Pamela Mishkin, Jack Clark, et al. Learning transferable visual models from natural language supervision. In *International conference on machine learning*, pp. 8748–8763. PMLR, 2021. [1](#), [4](#), [16](#)
- Leonardo FR Ribeiro, Yue Zhang, and Iryna Gurevych. Structural adapters in pretrained language models for amr-to-text generation. In *Proceedings of the 2021 Conference on Empirical Methods in Natural Language Processing*, pp. 4269–4282, 2021. [15](#)
- Anna Rohrbach, Lisa Anne Hendricks, Kaylee Burns, Trevor Darrell, and Kate Saenko. Object hallucination in image captioning. In *Proceedings of the 2018 Conference on Empirical Methods in Natural Language Processing*, pp. 4035–4045, 2018. [2](#), [3](#), [5](#), [17](#)
- Guillaume Sanchez, Honglu Fan, Alexander Spangher, Elad Levi, Pawan Sasanka Ammanamanchi, and Stella Biderman. Stay on topic with classifier-free guidance. *arXiv preprint arXiv:2306.17806*, 2023. [4](#), [15](#)
- Dustin Schwenk, Apoorv Khandelwal, Christopher Clark, Kenneth Marino, and Roozbeh Mottaghi. A-okvqa: A benchmark for visual question answering using world knowledge. In *European Conference on Computer Vision*, pp. 146–162. Springer, 2022. [2](#), [5](#), [7](#), [20](#)
- Hugo Touvron, Louis Martin, Kevin Stone, Peter Albert, Amjad Almahairi, Yasmine Babaei, Nikolay Bashlykov, Soumya Batra, Prajjwal Bhargava, Shruti Bhosale, et al. Llama 2: Open foundation and fine-tuned chat models. *arXiv preprint arXiv:2307.09288*, 2023. [16](#)
- Ramakrishna Vedantam, C. Lawrence Zitnick, and Devi Parikh. Cider: Consensus-based image description evaluation, 2015. [7](#), [16](#), [21](#)
- Bin Wang, Fan Wu, Xiao Han, Jiahui Peng, Huaping Zhong, Pan Zhang, Xiaoyi Dong, Weijia Li, Wei Li, Jiaqi Wang, et al. Vigc: Visual instruction generation and correction. *arXiv preprint arXiv:2308.12714*, 2023a. [1](#), [3](#)
- Junyang Wang, Yiyang Zhou, Guohai Xu, Pengcheng Shi, Chenlin Zhao, Haiyang Xu, Qinghao Ye, Ming Yan, Ji Zhang, Jihua Zhu, et al. Evaluation and analysis of hallucination in large vision-language models. *arXiv preprint arXiv:2308.15126*, 2023b. [1](#), [3](#)
- Xuezhi Wang, Jason Wei, Dale Schuurmans, Quoc V Le, Ed H Chi, Sharan Narang, Aakanksha Chowdhery, and Denny Zhou. Self-consistency improves chain of thought reasoning in language models. In *The Eleventh International Conference on Learning Representations*. [4](#)
- Peng Xu, Wenqi Shao, Kaipeng Zhang, Peng Gao, Shuo Liu, Meng Lei, Fanqing Meng, Siyuan Huang, Yu Qiao, and Ping Luo. Lvlm-ehub: A comprehensive evaluation benchmark for large vision-language models. *arXiv preprint arXiv:2306.09265*, 2023. [1](#)
- Zhengyuan Yang, Jianfeng Wang, Zhe Gan, Linjie Li, Kevin Lin, Chenfei Wu, Nan Duan, Zicheng Liu, Ce Liu, Michael Zeng, et al. Reco: Region-controlled text-to-image generation. In *Proceedings of the IEEE/CVF Conference on Computer Vision and Pattern Recognition*, pp. 14246–14255, 2023. [15](#)
- Qinghao Ye, Haiyang Xu, Guohai Xu, Jiabo Ye, Ming Yan, Yiyang Zhou, Junyang Wang, Anwen Hu, Pengcheng Shi, Yaya Shi, et al. mplug-owl: Modularization empowers large language models with multimodality. *arXiv preprint arXiv:2304.14178*, 2023. [1](#), [3](#), [4](#), [16](#)
- Shukang Yin, Chaoyou Fu, Sirui Zhao, Tong Xu, Hao Wang, Dianbo Sui, Yunhang Shen, Ke Li, Xing Sun, and Enhong Chen. Woodpecker: Hallucination correction for multimodal large language models. *arXiv preprint arXiv:2310.16045*, 2023. [1](#), [3](#), [5](#), [6](#), [7](#), [15](#), [18](#), [24](#)

- 
- Tianyu Yu, Yuan Yao, Haoye Zhang, Taiwen He, Yifeng Han, Ganqu Cui, Jinyi Hu, Zhiyuan Liu, Hai-Tao Zheng, Maosong Sun, et al. Rlhf-v: Towards trustworthy mllms via behavior alignment from fine-grained correctional human feedback. In *Proceedings of the IEEE/CVF Conference on Computer Vision and Pattern Recognition*, pp. 13807–13816, 2024. [1](#)
- Bohan Zhai, Shijia Yang, Chenfeng Xu, Sheng Shen, Kurt Keutzer, and Manling Li. Halle-switch: Controlling object hallucination in large vision language models. *arXiv e-prints*, pp. arXiv–2310, 2023. [3](#), [7](#)
- Hanqing Zhang, Haolin Song, Shaoyu Li, Ming Zhou, and Dawei Song. A survey of controllable text generation using transformer-based pre-trained language models. *ACM Computing Surveys*, 56(3): 1–37, 2023a. [15](#)
- Renrui Zhang, Dongzhi Jiang, Yichi Zhang, Haokun Lin, Ziyu Guo, Pengshuo Qiu, Aojun Zhou, Pan Lu, Kai-Wei Chang, Peng Gao, et al. Mathverse: Does your multi-modal llm truly see the diagrams in visual math problems? *arXiv preprint arXiv:2403.14624*, 2024. [1](#)
- Zhuosheng Zhang, Aston Zhang, Mu Li, Hai Zhao, George Karypis, and Alex Smola. Multimodal chain-of-thought reasoning in language models, 2023b. [2](#), [3](#)
- Yiyang Zhou, Chenhang Cui, Jaehong Yoon, Linjun Zhang, Zhun Deng, Chelsea Finn, Mohit Bansal, and Huaxiu Yao. Analyzing and mitigating object hallucination in large vision-language models. *arXiv preprint arXiv:2310.00754*, 2023. [1](#), [2](#), [3](#), [7](#), [15](#), [17](#), [24](#)
- Yiyang Zhou, Chenhang Cui, Rafael Rafailov, Chelsea Finn, and Huaxiu Yao. Aligning modalities in vision large language models via preference fine-tuning. *arXiv preprint arXiv:2402.11411*, 2024. [1](#)
- Deyao Zhu, Jun Chen, Xiaoqian Shen, Xiang Li, and Mohamed Elhoseiny. Minigt-4: Enhancing vision-language understanding with advanced large language models. *arXiv preprint arXiv:2304.10592*, 2023. [1](#), [3](#)

---

## A ETHICS STATEMENT

This paper introduces research aimed at advancing the field of Large Language Models. We are confident that our work will contribute to significant social benefits, particularly by enhancing the accountability of LLMs through the reduction of hallucinatory outputs. Our proposed method, MARINE, holds the potential to improve the fairness of LLM interactions by effectively reducing biased hallucinations. To the best of our knowledge, we have not identified any negative effects associated with our research that merit highlighting in this discussion.

## B REPRODUCIBILITY STATEMENT

We provide detailed descriptions of our experimental setups, datasets, models, codes in the supplementary materials to ensure the reproducibility of MARINE. The full experimental settings and hyperparameters are presented in Appendix D.

## C ADDITIONAL RELATED WORK

Controllable text generation (Prabhumoye et al., 2020; Hu & Li, 2021; Zhang et al., 2023a) has emerged as a vital research domain, focusing on the generation of natural sentences with controllable attributes such as persona (Prabhumoye et al., 2020; Hu & Li, 2021; Zhang et al., 2023a) and politeness (Niu & Bansal, 2018; Madaan et al., 2020). Among the various approaches, fine-tuning has been recognized as the most straightforward approach, achieved either through full fine-tuning (Li & Liang, 2021; Ouyang et al., 2022; Carlsson et al., 2022) or integrating tunable adaptors (Lin et al., 2021; Ribeiro et al., 2021). While fine-tuning has been effective in a wide range of applications, it is also expensive in computation as the size of LLMs is growing tremendously. Recently, there has been a development on controllable generation with diffusion models (Li et al., 2022; Lin et al., 2023b), extending to controllable text-to-image generation (Yang et al., 2023). Particularly, the use of classifier guidance (Dhariwal & Nichol, 2021) and classifier-free guidance (Ho & Salimans, 2021) has become prominent in refining the quality of generated outputs. Most recently, Sanchez et al. (2023) applied classifier-free guidance to language models in the *single-modal* setting to improve their performance at inference time. Our approach methodologically resembles classifier-free guidance for LVLMs’ text generation, while specifically addressing the *multi-modal* context and focusing on reducing hallucinations.

## D EXPERIMENT DETAILS

We conduct all of the experiments using 8 A6000 GPU with 48GB GPU memory. Each single experiment can be run on a single A6000 GPU. The hyperparameters for our method are fixed across tasks, with key settings including a guidance strength of 0.7, noise intensity for DETR at 0.95, a detection threshold for RAM++ of 0.68, and a greedy sampling approach with a random seed of 242.

### D.1 BASELINES.

In addition to comparing with the performance of the original LVLM sampling method, we also consider the following popular methods for mitigating hallucinations.

- *Greedy-Decoding*, which adopts the greedy sampling strategy, by generating tokens with the highest posterior probability to address hallucinations arising from.
- *LURE* (Zhou et al., 2023), which identifies and masks potentially hallucinated words and fine-tune a MiniGPT4 model to rectify object hallucinations in the generated descriptions.
- *LURE with Cutoff*. The original LURE method tends to generate long descriptions regardless of the provided instructions, which sometimes results in even worse performance as unnecessary information is included. Therefore, we also introduce a modified baseline, where we truncate the LURE’s output to match the length (in terms of the number of sentences) of the original generations.
- *Woodpecker* (Yin et al., 2023), which leverages GPT-3.5 to correct hallucinations in LVLM generation with five steps toward the correction.
- *VCD* (Leng et al., 2023), which distorts the image inputs to impose penalties on logit outputs.
- *OPERA* (Huang et al., 2023a), which penalizes logits to mitigate over-trust in beam-search decoding and adjusts token selection.

Lastly, the performance of MARINE improves in correlation with the advancement of the control guidance extractor used. Consequently, to demonstrate the potential upper bound of MARINE’s performance, we consider a version utilizing a ground-truth oracle extractor, which we denote as MARINE-Truth. Further details on model architectures, datasets and evaluation metrics are deferred to Appendix D.

## D.2 MODEL ARCHITECTURES

In Table 8, we provide detailed descriptions of the LVLM architectures used in our experiments. These LVLMs respectively leverage the pre-trained vision encoder of the models we listed, which are all based on the Vision Transformer (ViT) (Dosovitskiy et al., 2020) architecture.

Table 8: Details of the LVLM architectures that we used in our paper.

Model	Vision encoder	LLM
LLaVA (Liu et al., 2023d)	CLIP-L (Radford et al., 2021)	LLaMA-2-7B-Chat (Touvron et al., 2023)
LLaVA-v1.5 (Liu et al., 2023c)	CLIP-L-336px (Radford et al., 2021)	Vicuna-v1.5-7B (Chiang et al., 2023)
MiniGPT-v2 (Chen et al., 2023)	EVA-G (Fang et al., 2023)	LLaMA-2-7B-Chat (Touvron et al., 2023)
mPLUG-OWL2 (Ye et al., 2023)	CLIP-L (Radford et al., 2021)	LLaMA-2-7B (Touvron et al., 2023)
InstructBLIP (Dai et al., 2023a)	BLIP-2 (Li et al., 2023a)	Vicuna-v1.1-7B (Chiang et al., 2023)

## D.3 DESCRIPTIONS ABOUT ADDITIONAL METRICS

In Figure 2, we evaluate the text quality of the outputs generated with MARINE using general metrics as follows:

- *BLEU* (Papineni et al., 2002) measures how well the generated translation matches the reference translations in terms of n-gram overlap.
- *ROUGH-L* (Lin, 2004) measures the quality of a machine-generated summary by comparing it to one or more reference summaries.
- *CIDEr* (Vedantam et al., 2015) assesses the quality of image captioning models. It focuses on evaluating how well the generated captions align with human consensus.
- *SPICE* (Anderson et al., 2016) focuses on assessing the semantic similarity between the generated captions and reference captions.

## D.4 PROMPT TEMPLATES

For each query, we randomly select a prompt template from the available template list, as shown in Table 9.

Table 9: Details of the LVLM architectures that we used in our paper.

Template Type	Prompt Template
MARINE-intersec	<p>This image contains &lt;OBJECT_GROUNDING&gt;. Based on this, &lt;QUERY&gt;</p> <p>The image contains the following objects: &lt;OBJECT_GROUNDING&gt;. Given these detected objects, &lt;QUERY&gt;</p> <p>This image shows the following objects: &lt;OBJECT_GROUNDING&gt;. Using this information, &lt;QUERY&gt;</p> <p>The objects found in this image are: &lt;OBJECT_GROUNDING&gt;. Considering this list of objects, &lt;QUERY&gt;</p>
POPE task	<p>This image contains only the following objects: &lt;OBJECT_GROUNDING&gt;. Do not assume anything beyond these objects. Based solely on this list, &lt;QUERY&gt;</p> <p>The detected objects in the image are: &lt;OBJECT_GROUNDING&gt;. Answer based only on these objects. &lt;QUERY&gt;</p> <p>This image shows the following objects: &lt;OBJECT_GROUNDING&gt;. You must answer using only the objects in this list. Given these detected objects, &lt;QUERY&gt;</p> <p>The objects found in this image are limited to: &lt;OBJECT_GROUNDING&gt;. You should rely strictly on this list of objects and make no other guesses. Based on this, &lt;QUERY&gt;</p>
MARINE-union	<p>List of detected objects in the image:</p> <p>&lt;OBJECT_GROUNDING_A&gt;</p> <p>&lt;OBJECT_GROUNDING_B&gt;</p> <p>Based on the detected objects above, &lt;QUERY&gt;</p> <p>The most prominent objects detected are:</p> <p>&lt;OBJECT_GROUNDING_A&gt;</p> <p>&lt;OBJECT_GROUNDING_B&gt;</p> <p>Given these findings, &lt;QUERY&gt;</p> <p>The following objects were detected in the image:</p> <p>&lt;OBJECT_GROUNDING_A&gt;</p> <p>&lt;OBJECT_GROUNDING_B&gt;</p> <p>With this information, &lt;QUERY&gt;</p> <p>Here is a list of all objects detected in the image:</p> <p>&lt;OBJECT_GROUNDING_A&gt;</p> <p>&lt;OBJECT_GROUNDING_B&gt;</p> <p>Do not infer or hallucinate any additional objects. Using only the detected objects, &lt;QUERY&gt;</p>



## D.5 DETAILS OF BASELINES

Specifically, the hyperparameters for LURE (Zhou et al., 2023), VCD (Leng et al., 2023), OPERA (Huang et al., 2023a) are reported in Table 10, 11 and 12 respectively. We strictly followed the original implementations and default hyperparameters described in their papers to reproduce the results for each baseline.

Table 10: LURE (Zhou et al., 2023) Hyperparameter Settings

Parameters	Value
Uncertainty Threshold $\gamma$	0.9
Position Threshold $\iota$	0.8

Table 11: VCD (Leng et al., 2023) Hyperparameter Settings

Parameters	Value
Amplification Factor $\alpha$	1
Adaptive Plausibility Threshold	0.1
Diffusion Noise Step	500

Table 12: OPERA (Huang et al., 2023a) Hyperparameter Settings

Parameters	Value
Self-attention Weights Scale Factor $\theta$	50
Attending Retrospection Threshold	25
Beam Size	5
Attention Candidates	1
Penalty Weights	1

Table 13: MARINE Hyperparameter Settings. The settings are fixed depending on the question-answering tasks.

Parameters	Value
<i>Guidance</i>	
Guidance Strength	0.7
Noise Intensity for DETR	0.95
Detect Threshold for RAM++	0.68
<i>Generation</i>	
Max Token Length	64
Sampling	Greedy
Random Seed	242

Table 14: Batch size for LVLM generation is fixed across all experiments unless otherwise noted. To expedite the evaluation process, we employed the batched generation. We avoid the negative impact of batched generation by adopting left padding if the LVLM does not explicitly assign the padding strategy for inference.

Model	LLaVA	LLaVA-v1.5	MiniGPTv	mPLUG-Owl2	InstructBLIP
Batch Size	16	4	32	16	16

## D.6 EXPERIMENT SETTING FOR HALLUCINATION EVALUATIONS

Key factors that potentially affect the hallucination evaluation outcomes, including the evaluation dataset and prompt template, LVLM’s sampling strategy and batched generation techniques, and guidance strength, are detailed in this section. The hyper-parameters setting for MARINE and overall experiment settings are shown in Table 13 and 14.

**Experiment setting for CHAIR evaluation.** We adopt the same prompt “Generate a short caption of the image.” as utilized by Li et al. (2023b). The hyperparameters are fixed, including a guidance strength of 0.7, noise intensity for DETR at 0.95, a detection threshold for RAM++ of 0.68, a maximum token length of 64, and a greedy sampling approach with a random seed of 242. For the calculation of CHAIR metrics, we referenced the 80 object categories annotated in the MSCOCO dataset, following Rohrbach et al. (2018). Besides, we employed the synonym list from Lu et al. (2018) to align synonymous words in the generated text with MSCOCO object categories. Additionally, due to the cost considerations associated with the GPT-3.5 API, we limited our analysis to 200 samples for Woodpecker correction for each model and reported the result in Table 1.

**Experiment setting for POPE evaluation.** POPE is a flexible approach to evaluating hallucinations in LVLMs, which formulates a binary classification task by prompting LVLMs with questions such as “Is there a keyboard in this image?” to answer “yes” or “no”. Following Li et al. (2023b), we created 3000 POPE questions across three datasets—500 images each from MSCOCO, A-OKVQA, and GQA for the POPE evaluation. We reported the adversarial settings in Table 2, the most challenging setting, which constructs POPE questions from the top-k most frequently co-occurring but absent objects. Additionally, in Table 4, we reported the average scores under random, popular, adversarial settings across MSCOCO, A-OKVQA, and GQA datasets. The full POPE results are in Table 15.

Similarly, we constrained our analysis to 200 samples for Woodpecker correction for each model due to the high costs associated with the GPT API. The outcomes of this analysis are detailed in Table 2.

**Experiment setting for GPT-4V-aided evaluation.** The GPT-4V-aided evaluation compares the outputs of two LVM assistants using GPT-4V as a judge. We prompted GPT-4V to assess the quality of the generated outputs, scoring them out of 10 in two aspects:

- *Accuracy*: how accurately each assistant describes the image;
- *Detailedness*: the richness of necessary details in the response.

As shown in Figure 4, the assessment prompt template we used is slightly different from that of Yin et al. (2023). Specifically, we include the original question for a task-orientated evaluation and exclude prompts that describe Woodpecker-specific output formats like object bounding boxes. Examples of the GPT-4V-aid evaluation responses are illustrated in Figure 5 and 6. Besides, a fixed guidance strength of 0.5 was used in the evaluations in Table 3. Utilizing the gpt-4-1106-vision-preview, all final experiments were conducted between 01/01/2024-01/30/2024. As OpenAI continues to update its API, accessing different versions may result in slightly different values.

**Experiment setting for ablation study.** To explore different methods of integrating image-grounding models, we investigate the intersection and union of detected objects, with integration based on synonyms using the NLTK package.

To quantitatively assess the influence of guidance strength, we varied it from 0 to 1, as shown in Figure 8. These quantitative experiments were conducted using the same setting as those in CHAIR evaluation. For qualitative analysis, exemplified in Figure 11 and 8, we selected guidance strength from a recommended range of  $\gamma \in (0.3, 0.7)$ .

**Prompt**  
 You are required to score the performance of two AI assistants in describing a given image. You should pay extra attention to the hallucination, which refers to the part of descriptions that are inconsistent with the image content, such as claiming the existence of something not present in the image.  
 Please rate the responses of the assistants on a scale of 1 to 10, where a higher score indicates better performance, according to the following criteria:  
 1: Accuracy: whether the response is accurate with respect to the image content. Responses with fewer hallucinations should be given higher scores.  
 2: Detailedness: whether the response is rich in necessary details. Note that hallucinated descriptions should not count as necessary details.  
 Please output a single line for each criterion, containing only two values indicating the scores for Assistant 1 and 2, respectively. The two scores are separated by a space. Following the scores, please provide an explanation of your evaluation, avoiding any potential bias and ensuring that the order in which the responses were presented does not affect your judgment."

Please score the performance of two AI assistants in describing a given image following the given question.

Question:  
 {question}

Assistant 1:  
 {answer 1}

Assistant 2:  
 {answer 2}

Output format:  
 Accuracy:  
 Scores of the two answers:  
 Reason:

Detailedness:  
 Scores of the two answers:  
 Reason:

Figure 4: Prompt template for GPT-4V-aided evaluation. {question} is the original instruction; {answer 1} is the original response, and {answer 2} is the response generated by the LVM using MARINE-DETR with a guidance strength of 0.5.

**Prompt**

**Question:**

Can you elaborate on the elements of the picture provided?

**Assistant 1 (LLaVA-v1.5):**

The image features a desk with various items on it. There is a bookshelf with a few books, including a prominent one titled "Administrative Law". A blue and white tie is placed on the desk, adding a touch of color and formality to the scene. A pair of sunglasses is also resting on the desk, possibly belonging to someone who was recently there.

In addition to the books and tie, there is a cup and an apple on the desk, indicating that the person might have been enjoying a snack or drink while working or studying. A teddy bear is also present in the scene sitting on the desk, and adding a playful touch to the setting.

**Assistant 2 (LLaVA-v1.5 w/ MARINE):**

The image features a desk with various items on it. There is a book, possibly a law book, positioned on the left side of the desk. A blue and white tie is placed next to the book, adding a touch of color to the scene. On the right side of the desk, there is an apple, possibly a Granny Smith apple, and a pair of sunglasses.

Additionally, there is a stuffed teddy bear located at the top right corner of the desk, giving the scene a cozy and personal touch. A baseball glove is also present in the image, suggesting that the owner might have an interest in sports.



**GPT-4V Evaluation**

**Accuracy:**

Scores of the two answers: 4 7

**Reason:** Both assistants mention items that are present in the image, such as the book with the title "Administrative Law," the tie, the apple, the sunglasses, and the teddy bear. Assistant 1 hallucinates the presence of a cup, which is not visible in the image. Assistant 2 inaccurately describes the presence of a baseball glove, which is not in the image; the item mistaken for a glove is actually part of the teddy bear's outfit. Assistant 2 also avoids mentioning the specific title of the book, even though it is visible in the image.

**Detailedness:**

Scores of the two answers: 5 6

**Reason:** Assistant 1 provides a more detailed description of the scene by elaborating on the potential reasons for the items' presence, such as the person enjoying a snack or the teddy bear adding a playful touch. However, the mention of a cup, which is not in the image, detracts from the quality of the response. Assistant 2 provides a sufficient amount of detail without over-elaborating and makes a specific guess about the type of apple. However, the incorrect mention of a baseball glove and the lack of details about the book titles compared to Assistant 1 result in a slightly lower score.

Figure 5: An example of GPT-4V-aided evaluation on a detailed question.

**Prompt**

**Question:**

What might be the purpose of this table arrangement?

**Assistant 1 (LLaVA-v1.5):**

The purpose of this table arrangement might be to create a comfortable and productive workspace. The table features a pair of sunglasses, a book, and an apple, which are essential items for reading, relaxation and snacking. The presence of the book and sunglasses suggests that the person might be taking a break from reading or working on a project, while the apple provides a healthy snack option. The combination of these items on the table indicates that the person values both work and relaxation, aiming to create a balance between the two.

**Assistant 2 (LLaVA-v1.5 w/ MARINE):**

The purpose of this table arrangement appears to be a combination of work and leisure. The presence of books, a sunglasses, a tie, and an apple suggests that the person using this space may be engaged in work or study, as indicated by the books. Additionally, the apple and sunglasses indicate that the person might be taking a break, enjoying a snack, or preparing for a more relaxed activity. The presence of the teddy bear adds a touch of playfulness and personalization to the setting, creating a cozy and inviting atmosphere.

**GPT-4V Evaluation**

**Accuracy:**

Scores of the two answers: 6 7

**Reason:** Both Assistants made a few errors in their descriptions. Assistant 1 incorrectly states that there's a book on the table, which is ambiguous; technically, the books are not on the table but more likely on a shelf next to it and the tie isn't mentioned, which is a significant element in the image. Assistant 2 correctly recognizes the presence of books, a tie, sunglasses, and an apple, along with the teddy bear dressed in a sports jersey. However Assistant 2 also refers to books in a slightly ambiguous way, implying they are on the table, and incorrectly describes the sunglasses as "a sunglasses" which is grammatically incorrect and could slightly mislead the context.

**Detailedness:**

Scores of the two answers: 6 7

**Reason:** Assistant 1 provides an explanation of the potential purpose of the table arrangement but misses out mentioning the tie and teddy bear both of which add context to the scenario depicted. The description lacks detail on the actual arrangement and how it specifically suggests a mixture of work and leisure. Assistant 2 includes more elements in the description, such as the tie and teddy bear, adding to the detail and mentioning relaxation and personalization, which gives a slightly better insight into the purpose of the table arrangement, but their response could also be more nuanced by acknowledging the role of each item.



Figure 6: An example of GPT-4V-aided evaluation on a complex question.

## D.7 EXPERIMENT SETTING ON OTHER VISION-LANGUAGE TASKS

**Experiment setting for text quality analysis.** For text quality analysis, we adopted 90 visual questions from the LLaVA-QA90 task (including conversations, visual perceptions, and complex reasoning subtasks), and randomly selected 50 MSCOCO images for image captioning task. Following Liu et al. (2023d), we adopted the response generated by text-only GPT-4 (0314) with the context captions/boxes provided. answers given by GPT-4 as references for LLaVA-QA90 task and used image captions provided in MSCOCO annotations as references for image captioning task.

In Table 16 and Table 17, we present a detailed evaluation on the image captioning task for both MSCOCO and LLaVA-QA90 using metrics including BLEU, ROUGE, CIDEr and SPICE. The corresponding figure result is shown in Figure 2.

**Experiment setting for latency analysis.** We compared our method with existing baselines in terms of the trade-off between inference cost and the effectiveness of reducing object hallucinations, as shown in Table 5. For post-correction baselines such as Woodpecker and LURE, we first prompted LLaVA (llava-llama-2-7b-chat-lightning-preview) to generate captions and then measure the latency of generating the corrected outputs. The total latency for post-correction baselines includes both the generation and correction processes. For decoding methods such as VCD, OPERA and our method, we measured the latency of LLaVA generating captions directly.

We prompted the models with “Generate a short caption of the image.” on 500 MSCOCO images with a batch size of 1 and a maximum token length of 64, without any stopping criteria, using a single A6000 GPU. Then latency was calculated as the ratio of the number of output tokens and encoding and generation time.

Table 15: Detailed POPE (Li et al., 2023b) results on three datasets (MSCOCO (Lin et al., 2014), A-OKVQA (Schwenk et al., 2022), GQA (Hudson & Manning, 2019)).

Dataset	Type	Model	w/MARINE	Accuracy ↑	Precision ↑	Recall ↑	F1 ↑	Yes(%)
MSCOCO	Adversarial	LLaVA	✗	51.8	50.9	99.5	67.4	97.7
			✓	66.9	61.7	89.1	72.9	72.3
		mPLUG-Owl2	✗	72.5	65.5	94.9	77.5	72.4
			✓	82.8	83.4	82.0	82.7	49.2
	Popular	LLaVA	✗	52.4	51.2	99.8	67.7	97.4
			✓	71.3	65.8	88.9	75.6	67.5
		mPLUG-Owl2	✗	75.8	68.7	94.9	79.7	69.0
			✓	85.6	88.4	82.0	85.1	46.4
	Random	LLaVA	✗	58.3	54.5	99.7	70.5	91.4
			✓	78.5	73.4	89.3	80.6	60.8
		mPLUG-Owl2	✗	81.8	75.2	94.9	83.9	63.1
			✓	88.1	93.4	81.9	87.3	43.9
A-OKVQA	Adversarial	LLaVA	✗	50.0	50.0	99.5	66.6	99.5
			✓	56.3	53.6	94.3	68.3	88.1
		mPLUG-Owl2	✗	62.5	57.3	98.1	72.3	85.6
			✓	74.4	68.8	89.3	77.7	64.9
	Popular	LLaVA	✗	50.1	50.1	99.8	66.7	99.7
			✓	63.0	58.0	94.5	71.9	81.6
		mPLUG-Owl2	✗	69.1	62.1	97.9	76.0	78.9
			✓	82.5	78.8	89.1	83.6	56.5
	Random	LLaVA	✗	55.4	52.8	99.8	69.1	94.4
			✓	73.7	66.7	94.7	78.3	71.0
		mPLUG-Owl2	✗	77.2	69.2	98.2	81.2	71.0
			✓	89.2	89.2	89.3	89.2	50.1
GQA	Adversarial	LLaVA	✗	50.3	50.1	99.8	66.8	99.5
			✓	54.4	52.5	93.8	67.3	89.4
		mPLUG-Owl2	✗	68.4	63.0	98.2	75.6	79.8
			✓	76.0	73.6	81.2	77.2	55.2
	Popular	LLaVA	✗	50.1	50.0	99.8	66.7	99.7
			✓	58.7	55.1	94.3	69.5	85.5
		mPLUG-Owl2	✗	70.6	63.8	94.9	76.3	74.4
			✓	77.6	75.6	81.3	78.4	53.8
	Random	LLaVA	✗	55.7	53.0	99.8	69.2	94.1
			✓	74.3	67.3	94.8	78.7	70.5
		mPLUG-Owl2	✗	82.0	75.2	95.5	84.1	63.5
			✓	86.8	91.5	81.3	86.1	44.4

Table 16: Performance on general metrics for the image captioning task, including BLEU (Papineni et al., 2002), ROUGE-L (Lin, 2004), CIDEr (Vedantam et al., 2015) and SPICE (Anderson et al., 2016) scores(%).

Model	w/MARINE	BLEU_1 (↑)	BLEU_2 (↑)	BLEU_3 (↑)	BLEU_4 (↑)	ROUGE_L (↑)	CIDEr (↑)	SPICE (↑)
LLaVA	✗	14.06	7.12	3.72	1.90	22.06	0.08	16.77
	✓	18.59	9.96	5.47	3.04	26.02	0.21	20.58
mPLUG-Owl2	✗	39.91	25.16	16.57	11.24	36.26	1.05	26.82
	✓	39.51	24.37	15.93	10.70	36.01	1.03	27.42

Table 17: Performance on general metrics for the LLaVA-QA90 task, including BLEU (Papineni et al., 2002), ROUGE-L (Lin, 2004), CIDEr (Vedantam et al., 2015) and SPICE (Anderson et al., 2016) scores(%).

Model	w/MARINE	BLEU_1 (↑)	BLEU_2 (↑)	BLEU_3 (↑)	BLEU_4 (↑)	ROUGE_L (↑)	CIDEr (↑)	SPICE (↑)
LLaVA	✗	21.02	12.91	8.79	6.41	32.30	0.93	31.36
	✓	23.37	14.39	9.59	6.83	33.81	0.99	31.91
mPLUG-Owl2	✗	44.50	28.57	19.58	14.43	40.24	1.46	40.51
	✓	45.82	28.87	19.24	13.70	38.54	1.29	38.70

## E FURTHER MODEL PERFORMANCE ANALYSIS

### E.1 EXAMPLES OF MARINE’S GUIDED GENERATION.

In Figure 7, we provide specific generation examples of LLaVA based on queries from different tasks, with or without MARINE. In the first example, LLaVA incorrectly identifies a white chair in the image, an instance of hallucination as the object present is a white bird instead. In contrast, MARINE successfully mitigates this hallucination, correctly guiding the the model to recognize the object as a white bird. Similarly, in the second example, LLaVA erroneously state that the skateboard rider is holding onto the trucks. With MARINE, the model’s response is more accurate, focusing on verifiable visual elements and correctly stating that the person is standing on the skateboard without introducing non-existent details.

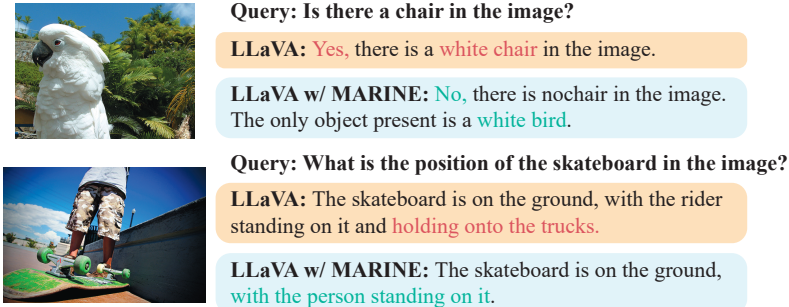


Figure 7: Examples of hallucination mitigation by our proposed MARINE across multiple tasks: POPE on the GQA dataset, LLaVA-QA90 task on the MSCOCO dataset, and image captioning. Hallucinated objects generated by LLaVA are highlighted in red.

### E.2 EFFECT OF MARINE ON LOGIT DISTRIBUTION.

In Figure 8, we illustrate a specific example that shows how MARINE influences the logit distribution of LLaVAs during text generation. Specifically, MARINE is observed to selectively target the potential hallucinated tokens, reducing their original probabilities to mitigate the risk of hallucination in the generated text. For instance, in the provided example, the probability of “fork” is significantly lowered with MARINE, which would have originally resulted in a hallucinated object. Conversely, standard language elements such as “various”, an adjective describing the overall image context, and “with”, a crucial preposition, maintain their original probabilities. This selective nature of modulation by MARINE ensures coherent and contextually relevant text generation that adheres to the instruction while effectively reducing hallucinations.

### E.3 DISCUSSION ON FINE-TUNING METHODS.

The examples depicted in Figure 9 illustrate that LURE, at times, fails to adhere to the given instructions when correcting LLaVA generations. Despite receiving concise image descriptions generated based on instructions for short responses, LURE predominantly overwrites them with excessively long responses that contain information irrelevant to the instruction. Furthermore, LURE fails to adequately address the binary question format of POPE, as LURE fixates on extended descriptions without responding with “yes” or “no”, making its evaluation using POPE impractical. This issue can be prevalent in small-scale fine-tuning methods, where the limited variety of the specifically tailored fine-tuning dataset harms the model’s performance on other tasks. In contrast, the training-free approach of MARINE demonstrates effective mitigation of hallucinations across a variety of question formats.

### E.4 EXTENDED ANALYSIS IN ABLATION STUDY

Additional experimental results explore the noise intensity of object grounding features, which are examined across LLaVA, InstructBLIP, and mPLUG-Owl2, with findings presented in Figures 10, 12, and 13.

This variation is achieved by implementing four confidence thresholds (0.5, 0.7, 0.9, and 0.95) in the DETR model predictions (with MARINE-Truth serving as an ideal reference), where higher thresholds correspond to lesser, yet higher-quality, visual information. Our findings highlight two significant insights. Firstly, an increase in the quality of visual information correlates with a noticeable decrease in hallucinations produced by the LLaVAs. A lower threshold, which allows for more visual information but also includes noisier content, could potentially result in an increased occurrence of

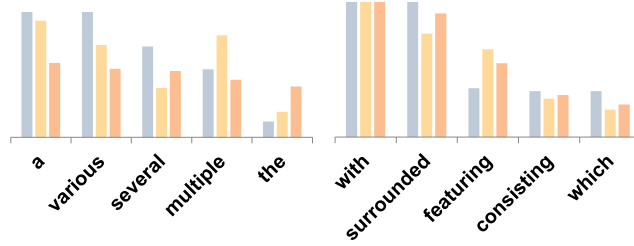
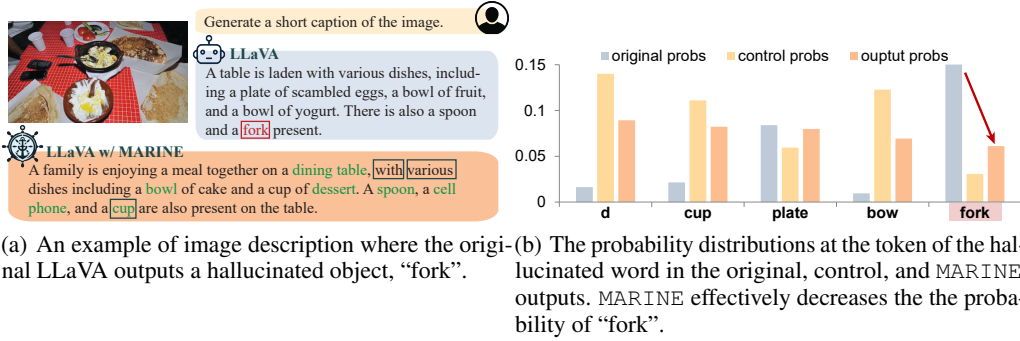


Figure 8: This sample shows how MARINE controls logit distributions to mitigate hallucinations like “fork” while preserving the probabilities of “with”, “various” during generation.

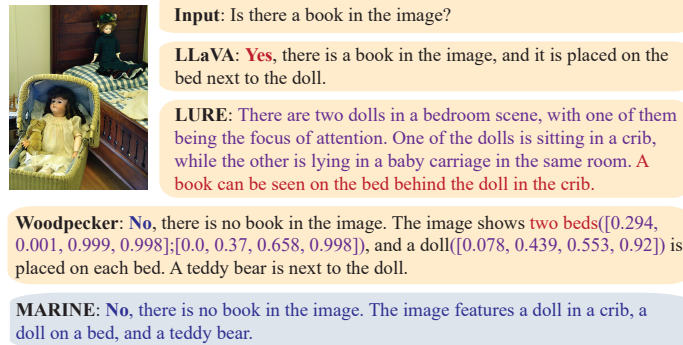


Figure 9: Example responses to an image-question pair. The LURE-corrected output deviates from the original question, offering irrelevant descriptions without directly addressing the query. Woodpecker hallucinates the existence of two beds while there is only one bed in the figure. In contrast, MARINE maintains the original answer’s style and adheres to the user’s instruction while eliminating hallucination.

hallucinations. Furthermore, lower-quality visual information is associated with enhanced Recall. This suggests that LVLMs under guidance, despite the presence of noisy visual inputs, tend to focus more on the visual details (i.e., objects), resulting in more elaborate descriptions.

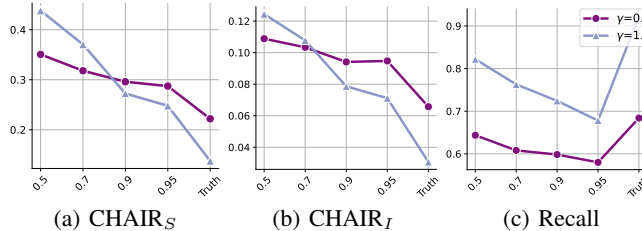


Figure 10: LLaVA’s performance on CHAIR according to different noise intensity of object grounding features in MARINE. We consider four confidence thresholds (0.5, 0.7, 0.9, and 0.95) for DETR to vary the noise intensity.

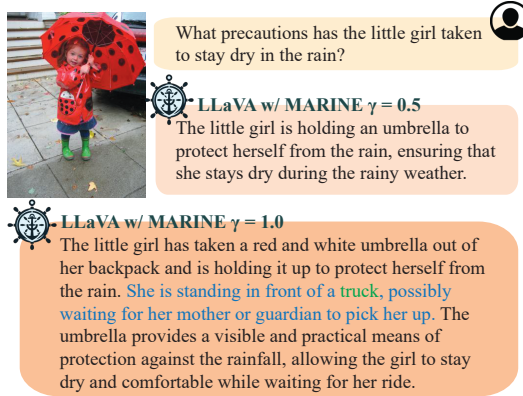


Figure 11: An example of the negative impact of excessive guidance on LLaVA’s ability to follow instructions accurately. While the response with  $\gamma = 1$  identifies more existing objects, it introduces irrelevant information to the instruction.

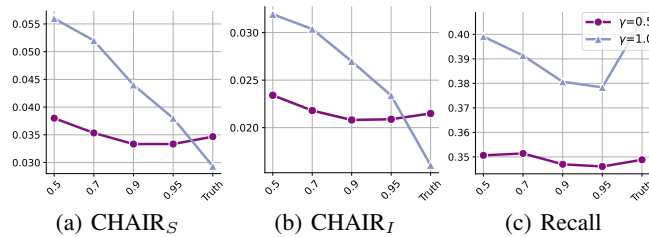


Figure 12: InstructBLIP’s performance on CHAIR according to different noise intensity of object grounding features in MARINE. We consider four confidence thresholds (0.5, 0.7, 0.9, and 0.95) for DETR to vary the noise intensity, with MARINE-Truth serving as an ideal reference.

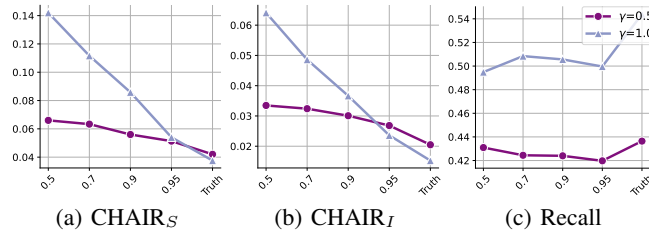


Figure 13: mPLUG-Owl2’s performance on CHAIR according to different noise intensity of object grounding features in MARINE. We consider four confidence thresholds (0.5, 0.7, 0.9, and 0.95) for DETR to vary the noise intensity, with MARINE-Truth serving as an ideal reference.

### E.5 MORE CASE STUDIES

In Figures 5 and 6, we present examples of GPT-4V-aided evaluations based on the outputs of LLaVA-v1.5 and LLaVA-v1.5 with MARINE. In Figures 14, 15, 16, 17, and 18, we present examples of the outputs from LURE (Zhou et al., 2023), Woodpecker (Yin et al., 2023) and MARINE on different tasks further validate our arguments in the paper.



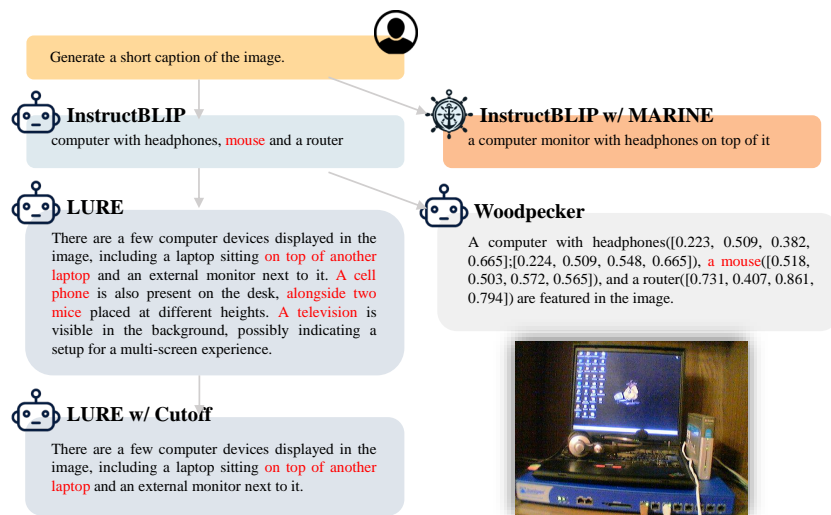


Figure 14: A comparison of responses from baseline models and our MARINE in an image description task. It illustrates MARINE’s superior ability to reduce hallucinations, in contrast to LURE and Woodpecker, which fail to effectively address hallucinations and sometimes even increase hallucinated content. This example highlights the strengths of our correct-during-generation framework over post-correction approaches, showcasing its efficiency, preservation of original style, and enhanced adherence to instructions.

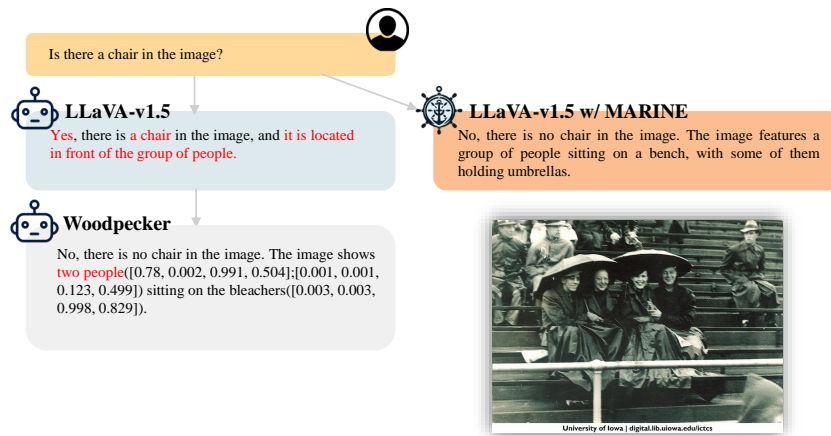


Figure 15: A comparison of responses from Woodpecker and our MARINE in POPE “yes-or-no” task.

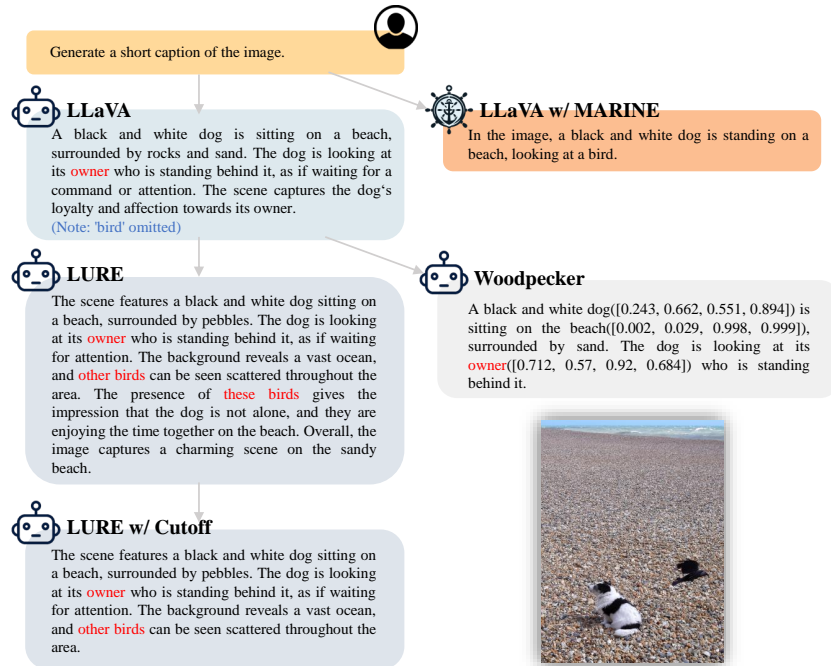


Figure 16: A comparison of responses from baseline models and our MARINE in an image description task. MARINE effectively reduces hallucinations and accurately includes the previously omitted object, 'bird', enhancing the description with essential details.

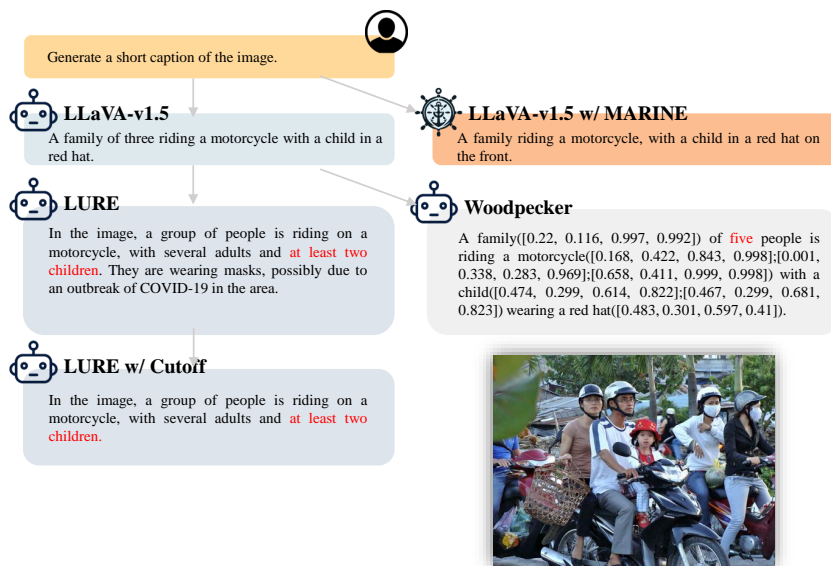


Figure 17: A comparison of responses from baseline models and our MARINE in an image description task.

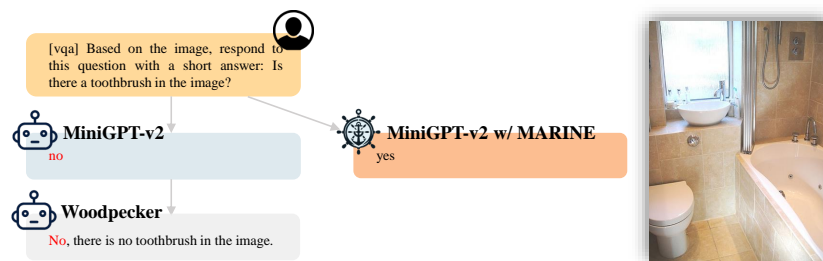


Figure 18: A comparison of responses from baseline models and our MARINE in POPE “yes-or-no” task. MiniGPT-v2 provides a concise response without referencing any objects. Under these circumstances, Woodpecker is unable to perform corrections via GPT-3.5 due to missing visual details. MARINE, however, successfully corrects the response while retaining MiniGPT-v2’s style.